A Convenient Analytical Framework for Electromagnetic Scattering from Composite Targets

W. Fuscaldo[1,2], A. Di Simone[2,3], L. M. Millefiori[2], A. Iodice[3], P. Braca[2], P. K. Willett[4]

[1]Department of Information Engineering, Electronics, and Telecommunications, Sapienza University of Rome, 00184 Rome, Italy.
[2]NATO-STO Centre for Maritime Research and Experimentation, 19126 La Spezia, Italy.
[3]Department of Information Technology and Electrical Engineering, University of Naples "Federico II", 80125 Naples, Italy.
[4]Department of Electrical and Computer Engineering, University of Connecticut, Storrs, CT 06269 USA.

Key Points:

- Explicit formulation of the scattering matrix under Kirchhoff Approximation in arbitrary geometry
- Analytical expressions of the scattering matrix under Geometrical Optics and Physical Optics approximations
- Application to canonical composite targets of practical interest

Corresponding author: W. Fuscaldo, walter.fuscaldo@uniroma1.it

Corresponding author: A. Di Simone, alessio.disimone@unina.it

Abstract

This paper furnishes a convenient theoretical framework for the analytical evaluation of the bistatic scattering coefficients, under the Kirchhoff approximation (KA) in electromagnetics. Starting from the KA, specific results under the geometrical optics and physical optics approximations are furnished, along with the backscattering geometry. The main aim is to provide closed-form expressions of the scattering matrix that are suited to scenarios where multiple-bounce scattering comes into play and/or surfaces with arbitrary unit normal are present. This is accomplished by addressing the following objectives: 1) to provide an explicit formulation of the scattering matrix under KA in terms of the incident and scattered unit wavevectors; 2) to provide a more generic derivation of the scattering matrix under the physical optics approximation by relaxing typical hypotheses regarding the geometry of the scattering problem; 3) to highlight some important symmetries of the scattering matrix under KA. It is shown that the scattering matrix under KA can conveniently be expressed in terms of few variables, thus greatly reducing the complexity of the theoretical derivation of the scattering matrix. Some benefits of the proposed formalism are illustrated in two application examples, where the problem is the analysis of the electromagnetic scattering from canonical composite targets. The canonical study cases demonstrate the evaluation of the scattering matrix in complex scenarios, such as maritime and urban environments, where multiple-bounce contributions and/or contributions from tilted surfaces come into play. Finally, comparisons with literature results allow for validating the proposed derivation and assessing its validity limits in practical applications.

1 Introduction

In remote sensing the information that can be retrieved from the processing of radar signals is consistently affected by the availability of accurate physical and mathematical models, which describe the interaction between the electromagnetic (EM) fields and the targets under investigation.

With the spread of passive bistatic radar (PBR) systems [*Griffiths*, 2014; *Cherniakov*, 2008; *Colone et al.*, 2009], as well as the use of reflectometry in global navigation satellite systems (GNSS-R) [*Jin and Komjathy*, 2010; *Jin et al.*, 2011; *Zuffada et al.*, 2015; *Zavorotny et al.*, 2014], the accurate modeling of electromagnetic scattering is made difficult due to their generic bistatic configurations. Moreover, in these contexts, radar signals may interact with composite targets in different environments such as urban areas, maritime scenarios and vegetation regions, where the mathematical complexity of the scattering problem depends on the desired degree of accuracy.

Most common remote sensing technologies operating at microwave frequencies comprise scatterometers, synthetic aperture radar (SAR), GNSS-R and PBR. A rigorous and quantitative analysis of remote sensing data in such scenarios may be fruitfully supported by an accurate modeling of the relationship between the scene parameters of interest and the sensor observables. To this end, the modeling rationale can be decomposed into two main steps: 1) the acquisition process, i.e., the set of procedures applied to measurements to obtain the final observable, e.g., a SAR image, a scatterometric or a delay-Doppler map; 2) the physical mechanisms that contribute to the measurement performed by the sensor. Concerning the first issue, accurate and well-established imaging models, which describe the data processing chain, have been developed in the literature, see [*Zavorotny and Voronovich*, 2000; *Franceschetti and Lanari*, 2018; *Clarizia et al.*, 2015; *Di Martino et al.*, 2018]. Such models provide a relationship between the sensor observable and the radar cross section (RCS) of the illuminated scene. The second step is devoted to the derivation of a suitable scattering model, i.e., a proper description of the relationship between the scene parameters of interest and the RCS. The combination of the imaging and scattering models provides the final link between the scene and sensor parameters and the acquired data.

Here we focus on the scattering models, since the RCS is demonstrated to be proportional to the final observable [*Clarizia et al.*, 2015; *Di Martino et al.*, 2018]. Closed-form expressions of RCS may greatly ease the retrieval procedure in inversion algorithms and the automatic processing by computer programs. However, the complexity of the interactions between the electromagnetic radiation and the media prevents the derivation of an exact solution to the scattering problem in realistic scenarios.

In this regard, scattering models have been suitably simplified in order to gain the mathematical treatability of the problem, while maintaining the required accuracy to capture the underlying physics of the problem. A typical example is that of the Kirchhoff approximation (KA) [*Hentschel and Zhu*, 2016; *Tsang et al.*, 1985; *Tsang and Kong*, 2001; *Ulaby et al.*, 1982; *Franceschetti*, 2013; *Franceschetti and Riccio*, 2007], which requires the operating wavelength to be much smaller than the surface mean radius of curvature of the scatterer, but allows for a great simplification of the scattering problem. As a consequence, at microwave frequencies, the theoretical framework of KA can conveniently be used for the numerical analysis of electromagnetic scattering problems in complex scenarios where multipath and shadowing phenomena are relevant, e.g., urban and maritime domains [*Franceschetti et al.*, 2002; *Iervolino et al.*, 2016; *Di Simone et al.*, 2017].

In this context, several efforts have attempted to provide analytical electromagnetic models for the detection of buildings [*Franceschetti et al.*, 2002] and ships [*Iervolino et al.*, 2016] in backscattering configuration. Nevertheless, the rise of PBR and other multistatic systems, e.g., GNSS-R, demands the development of accurate electromagnetic models in bistatic configuration, rather than in backscattering. In both cases, the received signals depend on the bistatic radar cross section (BRCS) [*Zavorotny et al.*, 2014], whose accurate estimation is a key aspect in many applications [*Clarizia et al.*, 2015].

Unfortunately, in the current literature there are few analytical models for the determination of RCS of composite targets [*Barrick*, 1970; *Tateiba et al.*, 2004; *El-Ocla and Tateiba*, 2008], even under the Geometrical Optics (GO) and the Physical Optics (PO) approximations. Several attempts have been made to find general and compact expressions for the bistatic scattering matrix starting from the more general framework of KA, but analytical formulas for the scattering coefficients are obtained only under the KA-GO approximation [*Stogryn*, 1967; *Jin and Lax*, 1990; *Elfouhaily et al.*, 2004].

In [*Barrick*, 1968; *Bass and Fuks*, 1979] the BRCS is evaluated under KA-GO, thus neglecting the non-coherent component of the scattering. In this regard, in [*Pierdicca et al.*, 2014] a simulator has been proposed, which accounts for both the coherent and non-coherent scattering components. In all these models [*Barrick*, 1968; *Bass and Fuks*, 1979; *Pierdicca et al.*, 2014], the BRCS is always expressed in terms of the scattering coefficients. However, these quantities have always to be calculated through the conventional theoretical framework outlined in classic books on microwave remote sensing (see, e.g., [*Tsang et al.*, 1985; *Tsang and Kong*, 2001; *Ulaby et al.*, 1982; *Franceschetti*, 2013; *Franceschetti and Riccio*, 2007; *Barrick*, 1970]).The final expressions provided in such literature are not suited to the analytical derivation of the scattering matrix of composite targets [*Franceschetti et al.*, 2002; *Iervolino et al.*, 2016; *Di Simone et al.*, 2017], nor they are sufficiently general. In particular, restricting hypotheses about the acquisition and the scattering geometry are made in [*Franceschetti et al.*, 2002] and [*Barrick*, 1970], respectively. As a consequence, they do not allow for a straightforward evaluation of the BRCS of such targets. Furthermore, in most of the available literarure [*Tsang et al.*, 1985; *Ulaby et al.*, 1982; *Franceschetti*, 2013; *Franceschetti and Riccio*, 2007; *Barrick*, 1970; *Tsang and Kong*, 2001], the scattering coefficients under KA are not expressed in terms of unit wavevectors and surface orientation; a feature that might be rather helpful for electromagnetic solvers.

In this work, we present an alternative theoretical framework for the evaluation of the bistatic scattering coefficients under KA. The proposed formalism is particularly suited to the evaluation of the scattering matrix in scenarios where multiple-bounce scattering comes

into play and/or surfaces with arbitrary unit normal are present. This is accomplished by addressing the following objectives: 1) to provide an explicit formulation of the scattering matrix under KA in terms of the incident and scattered unit wavevectors; 2) to provide generic expressions of the scattering matrix under the physical optics approximation by relaxing typical hypotheses regarding the geometry of the scattering problem; 3) to highlight some important symmetries of the scattering matrix under KA which ease its analytical derivation. Remarkably, no assumptions are applied to either the scattering surface orientation nor the wavevectors. In addition, the proposed formalism highlights interesting symmetries which are used for a straightforward derivation of the scattering matrix under KA.

Explicit analytical expressions under KA-GO, KA-PO, and the limiting backscattering (BS) case are derived to express the scattering coefficients in terms of the relative positions between the transmitter, the receiver, and the scatterer. The obtained formulas are compared with the current literature, when available. Indeed, it is worth to stress here that analytical formulas for the scattering coefficients under the KA-PO approximation have never been reported so far. As a result, once the geometry of acquisition is known, the proposed formulas allow for a direct calculation of the scattering matrix to be used in theoretical and numerical approaches to scattering problems. This is demonstrated by applying the proposed simplified framework to a composite target consisting of a smooth parallelepiped laying on a rough surface. The rationale for the theoretical derivation of the scattering matrix associated to a double-bounce scattering contribution is here presented. Finally, we show numerical results of the bistatic RCS of the considered target. Indeed, despite its essentially theoretical nature, this approach is sufficiently general to be applied in most of radar system simulators (e.g., [*Zavorotny et al.*, 2014; *Park et al.*, 2017; *Giangregorio et al.*, 2016; *Garrison*, 2016; *Arnold-Bos et al.*, 2007a,b]).

The paper is organized as follows. In Section 2 the conventional scattering model is briefly reviewed under the Kirchhoff approximation; its GO and the PO approximations are then presented as special cases of KA. In Section 3, the scattering matrix is suitably recast under KA in order to derive a rigorous theoretical framework which is able to deal with bistatic configurations. In Sections 4 and 5 analytical formulas are derived under the KA-GO and the KA-PO approximations, respectively. In Section 6 the relevant case of backscattering is presented. In Section 7, some benefits of the proposed formalism are illustrated in two canonical study cases, where the derivation of the scattering matrix in composite scenarios is presented. In Section 8, the proposed framework is compared with literature results. Finally, conclusions are drawn in Section 9.

2 Scattering Models under Kirchhoff Approximation

In this Section, we introduce the KA, a well-known and well-established surface-scattering theory [*Tsang et al.*, 1985; *Ulaby et al.*, 1982; *Franceschetti et al.*, 2002]. The KA requires that the scattering surface have gentle undulations with average horizontal dimension large with respect to the incident wavelength, and that the local radius of curvature be sufficiently large so that the surface appears as locally smooth [*Ulaby et al.*, 1982]. This hypothesis is expressed by the following conditions, which provides the domain of validity of KA for rough surfaces [*Ulaby et al.*, 1982]:

$$k\rho_{\mathrm{l}} > 6, \tag{1a}$$

$$\rho_{\mathrm{l}} > \sqrt{2.76\sigma_{\mathrm{h}}\lambda}, \tag{1b}$$

where $k = 2\pi/\lambda$ is the free-space wavenumber (λ being the operating wavelength), whereas ρ_{l} and σ_{h} are the correlation length and the height standard deviation characterizing the statistical representation of the rough surface.

Considering the geometry depicted in Fig. 1, the field $\underline{E}_{\mathrm{s}}$ scattered by a generic surface S at the interface between two different media can be expressed under the KA as (a time

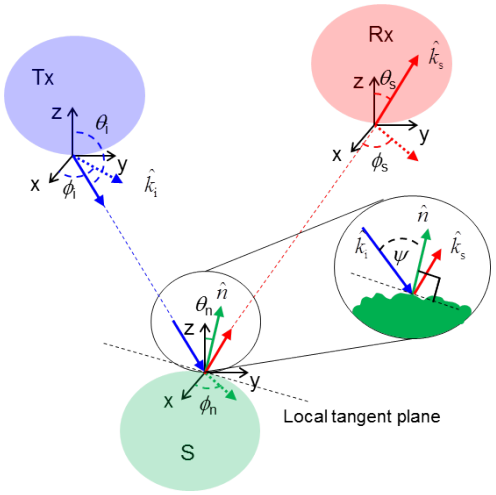

Figure 1. Geometry of a generic bistatic scattering scenario. The labels 'Tx', 'Rx', and 'S' stand for transmitter, receiver, and scatterer, respectively. Dashed lines represent the projections of the unit vectors onto the xy-plane.

dependence $e^{j\omega t}$ is understood):

$$\underline{E}_{\rm s}(\underline{r}) = \frac{jke^{jkr}}{4\pi r} E_0(\underline{\underline{I}} - \hat{k}_{\rm s}\hat{k}_{\rm s}) \iint_S \underline{F}(\hat{k}_{\rm i},\hat{e}_{\rm i},\hat{n}) e^{j(\underline{k}_{\rm i}-\underline{k}_{\rm s})\cdot\underline{r}'} d\underline{r}', \tag{2}$$

where $\underline{r}'$ is the surface point, and $\underline{r}$ the observation point in the far-field region (thus $r \sim |\underline{r}-\underline{r}'|$); $\underline{k}_{\rm i}$ and $\underline{k}_{\rm s}$ are the incident and the scattered wavevectors, respectively, $\hat{e}_{\rm i}$ is the polarization unit vector of the incident electric field $\underline{E}_{\rm i} = E_0\hat{e}_{\rm i}e^{j\underline{k}_{\rm i}\cdot\underline{r}'}$ (which is assumed to be a plane wave due to the far-field hypothesis), E_0 being an arbitrary amplitude factor, whereas $\hat{n}$ is the normal unit vector of the surface S [throughout the paper, unit vectors are identified with a hat $(\hat{\cdot})$]. The vector function $\underline{F}$ depends on the surface slopes and dielectric properties; its expression is given by [*Franceschetti et al.*, 2002]:

$$\begin{aligned} \underline{F}(\hat{k}_{\rm i},\hat{e}_{\rm i},\hat{n}) \;=\; & -(\hat{e}_{\rm i}\cdot\hat{q}_{\rm i})(\hat{n}\cdot\hat{k}_{\rm i})\hat{q}_{\rm i}(1-R_\perp) + (\hat{e}_{\rm i}\cdot\hat{p}_{\rm i})(\hat{n}\times\hat{q}_{\rm i})(1+R_{/\!/}) \\ & + (\hat{e}_{\rm i}\cdot\hat{q}_{\rm i})[\hat{k}_{\rm s}\times(\hat{n}\times\hat{q}_{\rm i})](1+R_\perp) + (\hat{e}_{\rm i}\cdot\hat{p}_{\rm i})(\hat{n}\cdot\hat{k}_{\rm i})(\hat{k}_{\rm s}\times\hat{q}_{\rm i})(1-R_{/\!/}), \end{aligned} \tag{3}$$

where $(\hat{p}_{\rm i},\hat{q}_{\rm i},\hat{k}_{\rm i})$ defines a local orthonormal system on the surface S with

$$\hat{q}_{\rm i} = \frac{\hat{k}_{\rm i}\times\hat{n}}{|\hat{k}_{\rm i}\times\hat{n}|}, \qquad\qquad \hat{p}_{\rm i} = \hat{q}_{\rm i}\times\hat{k}_{\rm i}, \tag{4}$$

whereas $R_{/\!/}$ and $R_\perp$ are the Fresnel coefficients for locally parallel $\hat{p}_{\rm i}$ and perpendicular $\hat{q}_{\rm i}$ polarizations, respectively, evaluated at the local incidence angle $\psi = \arccos(-\hat{k}_{\rm i}\cdot\hat{n}_{\rm s})$, thus $\psi\in[0,\pi/2]$. The dependence of $R_{/\!/}$ and $R_\perp$ on ψ is understood and omitted for clarity purposes.

At this point, it is convenient to define the horizontal (identified with the subscript 'h') and vertical (identified with the subscript 'v') polarization states for both the incident $\underline{E}_{\rm i}$ and the scattered $\underline{E}_{\rm s}$ electric fields

$$\hat{e}_{\rm ih} = \frac{\hat{k}_{\rm i}\times\hat{z}}{|\hat{k}_{\rm i}\times\hat{z}|}, \qquad\qquad \hat{e}_{\rm iv} = \hat{e}_{\rm ih}\times\hat{k}_{\rm i}, \tag{5a}$$

$$\hat{e}_{\rm sh} = \frac{\hat{k}_{\rm s}\times\hat{z}}{|\hat{k}_{\rm s}\times\hat{z}|}, \qquad\qquad \hat{e}_{\rm sv} = \hat{e}_{\rm sh}\times\hat{k}_{\rm s}, \tag{5b}$$

where $\hat{z}$ is the vertical unit vector of the cartesian reference frame $(\hat{x},\hat{y},\hat{z})$, as shown in Fig. 1. With these definitions at hand, we can suitably define a *local* scattering matrix $\underline{\underline{\tilde{S}}}(\underline{r}')$ as

$$\underline{\underline{\tilde{S}}}(\underline{r}') = \begin{pmatrix} \tilde{S}_{\mathrm{hh}}(\underline{r}') & \tilde{S}_{\mathrm{vh}}(\underline{r}') \\ \tilde{S}_{\mathrm{hv}}(\underline{r}') & \tilde{S}_{\mathrm{vv}}(\underline{r}') \end{pmatrix}, \tag{6}$$

where the generic element of the S-matrix is

$$\tilde{S}_{pq}(\underline{r}') = \left[(\underline{\underline{I}} - \hat{k}_{\mathrm{s}}\hat{k}_{\mathrm{s}})\underline{F}(\hat{k}_{\mathrm{i}},\hat{e}_{\mathrm{i}p},\hat{n}(\underline{r}')) \right] \cdot \hat{e}_{\mathrm{s}q}, \tag{7}$$

for $p,q \in \{\mathrm{h},\mathrm{v}\}$, so that the scattered electric field $\underline{E}_{\mathrm{s}}$ in (2) can be recast in terms of the horizontal (E_{sh}) and the vertical (E_{sv}) components in the following compact form:

$$\begin{bmatrix} E_{\mathrm{sh}} \\ E_{\mathrm{sv}} \end{bmatrix} = \frac{jke^{jkr}}{4\pi r} \iint_{\mathrm{S}} e^{j(\underline{k}_{\mathrm{i}} - \underline{k}_{\mathrm{s}})\cdot\underline{r}'} \underline{\underline{\tilde{S}}}(\underline{r}') d\underline{r}' \begin{bmatrix} E_{0\mathrm{h}} \\ E_{0\mathrm{v}} \end{bmatrix}, \tag{8}$$

$E_{0\mathrm{h}}$ and $E_{0\mathrm{v}}$ being the amplitudes of the horizontal and vertical components of the incident electric field $\underline{E}_{\mathrm{i}}$, respectively. The scattered field as expressed in either (2) or (8) does not allow for analytical solutions, unless further approximations and/or hypotheses are introduced [*Ulaby et al.*, 1982]. However, as long as the normal unit vector is fixed, i.e., $\hat{n}(\underline{r}') = \hat{n}$, the *local* scattering matrix $\underline{\underline{\tilde{S}}}(\underline{r}')$ no longer depends on $\underline{r}'$, thus allowing for the following simplification

$$\begin{bmatrix} E_{\mathrm{sh}} \\ E_{\mathrm{sv}} \end{bmatrix} = \frac{jke^{jkr}}{4\pi r} \underline{\underline{S}} \begin{bmatrix} E_{0\mathrm{h}} \\ E_{0\mathrm{v}} \end{bmatrix} I_{\mathrm{S}}, \tag{9}$$

where

$$I_{\mathrm{S}} = \iint_{\mathrm{S}} e^{j(k_i - k_s)\cdot\underline{r}'} d\underline{r}', \tag{10}$$

is the scattering integral, whereas $\underline{\underline{S}}$ is the *global* scattering matrix

$$\underline{\underline{S}} = \begin{pmatrix} S_{\mathrm{hh}} & S_{\mathrm{vh}} \\ S_{\mathrm{hv}} & S_{\mathrm{vv}} \end{pmatrix}, \tag{11}$$

with the generic element defined as:

$$S_{pq} = \left[(\underline{\underline{I}} - \hat{k}_s\hat{k}_s)\underline{F}(\hat{k}_{\mathrm{i}},\hat{e}_{\mathrm{i}p},\hat{n}) \right] \cdot \hat{e}_{\mathrm{s}q}. \tag{12}$$

It is worth noting here that the *local* scattering matrix $\underline{\underline{\tilde{S}}}(\underline{r}')$ accounts for the elementary contribution of the scattered field from any single facet (located at $\underline{r}'$) constituting the overall surface. Conversely, the scattering matrix $\underline{\underline{S}}$ accounts for the *global* contribution of the scattered field from the overall surface S. As is manifest by comparison of either (7) and (12), or (8) and (9), $\underline{\underline{S}}$ and $\underline{\underline{\tilde{S}}}(\underline{r}')$ coincide for $\hat{n}(\underline{r}') = \hat{n}$, being $\underline{\underline{\tilde{S}}}$ no longer dependent from $\underline{r}'$. Note that, throughout the paper, the subscripts p,q are intended as labels for the possible polarization states (viz., 'h', and 'v', for the horizontal and vertical polarization, respectively).

In this work, we thoroughly address the analytical evaluation of the *local* scattering matrix under KA. As specific cases of interest, we also propose simplified analytical expressions under the GO and the PO approximations, and finally under the backscattering (BS) hypothesis. To this purpose, it is worth recalling here that both the KA-GO and the KA-PO approximations allow for considering a fixed surface orientation, i.e., $\hat{n}(\underline{r}') = \hat{n}$, thus the expressions of $\underline{\underline{\tilde{S}}}(\underline{r}')$ coincide with those of $\underline{\underline{S}}$. It is worth recalling that the GO approximation is applicable also to rough surfaces with standard deviation of the surface heights large with respect to the wavelength, whereas the PO solution holds for surfaces with small slopes and height standard deviation much smaller than the wavelength [*Ulaby et al.*, 1982]. Such assumptions are introduced to evaluate the scattering integral in (10) in closed-forms but are not strictly required for the derivation of the scattering matrix which is the main focus of this work. In the next Subsections, the hypotheses underlying the KA-GO and the KA-PO approximations are briefly reviewed.

2.1 Geometrical Optics (GO) Approximation

As is known [*Franceschetti et al.*, 2002; *Ulaby et al.*, 1982], under the GO approximation, the main contributions to the scattered fields arise from the stationary phase points. Consequently, $\hat{k}_\mathrm{i}$, $\hat{k}_\mathrm{s}$, and $\hat{n}$ must obey the condition of specular reflection

$$\hat{k}_\mathrm{s} = \hat{k}_\mathrm{i} - 2(\hat{k}_\mathrm{i}\cdot\hat{n})\hat{n}. \tag{13}$$

For random surfaces (e.g., rough surfaces, where the roughness is described by a random variable), (13) fixes $\hat{n} = \hat{n}_\mathrm{s}$ with

$$\hat{n}_\mathrm{s} = \frac{\hat{k}_\mathrm{s} - \hat{k}_\mathrm{i}}{\sqrt{2}\sqrt{1-\hat{k}_\mathrm{i}\cdot\hat{k}_\mathrm{s}}}. \tag{14}$$

Note that (14) has been found from (13) by exploiting the following useful relations:

$$\hat{k}_\mathrm{s}\cdot\hat{n}_\mathrm{s} = -\hat{k}_\mathrm{i}\cdot\hat{n}_\mathrm{s} = \cos\psi, \tag{15a}$$

$$\hat{k}_\mathrm{i}\cdot\hat{k}_\mathrm{s} = 1 - 2\cos^2\psi, \tag{15b}$$

$$\cos\psi = \sqrt{(1-\hat{k}_\mathrm{i}\cdot\hat{k}_\mathrm{s})/2}, \tag{15c}$$

$$\hat{n}_\mathrm{s} = (\hat{k}_\mathrm{s} - \hat{k}_\mathrm{i})/(2\cos\psi). \tag{15d}$$

As a result, whatever the surface elevation model, deterministic or stochastic, under the KA-GO approximation the surface orientation is always fixed, and thus the *local* scattering matrix coincides with the scattering matrix, i.e., $\underline{\underline{\tilde{S}}}(\underline{r}') = \underline{\underline{S}}$. It is worth mentioning here that the domain of validity of KA-GO is determined by the following condition, in addition to (1a) and (1b), [*Ulaby et al.*, 1982]:

$$k^2\sigma_\mathrm{h}^2|(\hat{k}_\mathrm{i} - \hat{k}_\mathrm{s})\cdot\hat{z}|^2 > 10. \tag{16}$$

The condition in (16) ensures the applicability of the stationary phase method to the evaluation of the scattering integral in (10).

2.2 Physical Optics (PO) Approximation

As pointed out in [*Franceschetti et al.*, 2002], the PO approximation commonly refers to the KA, e.g. [*Barrick*, 1968]. Here, according to [*Franceschetti et al.*, 2002], the PO approximation is referred to the approximation of a random surface as the sum of a mean plane with a normal unit vector $\hat{n}_0$ and a superimposed roughness. Under the hypothesis of small roughness, $\underline{F}$ appearing in (2) can be expanded around $\hat{n}_0$, so that the zero-th order PO solution of the scattered fleld $\underline{E}_\mathrm{s}$ can still be expressed by (9). Throughout the paper, this will be referred to as the KA-PO approximation. Similar to KA-GO, the domain of validity of KA-PO is further restricted with respect to the KA in order to express the scattering integral in (10) in a closed form. Specifically, the series expansion of the integrand calls for a scattering surface with gentle ondulations. Concerning the scattering from rough surfaces, the following condition has to be satisfied in addition to (1a) and (1b) [*Ulaby et al.*, 1982]:

$$\sqrt{2}\sigma_\mathrm{h}/\rho_\mathrm{l} < 0.25. \tag{17}$$

Evidently, for deterministic surfaces, KA consistently leads to the use of the simplified scattering model expressed by (9), whereas for random surfaces KA-PO is needed. Therefore, either if the surface is deterministic, or if it is random, under KA-PO approximation, the surface orientation is always fixed, and thus the *local* scattering matrix coincides with the scattering matrix, i.e., $\underline{\underline{\tilde{S}}}(\underline{r}') = \underline{\underline{S}}$.

As a final comment, we should note that for KA-PO approximation we will present two relevant cases of $\hat{n} = \hat{z}$ and $\hat{n}\cdot\hat{z} = 0$, representing, e.g., the case of a *ground* and that of a

wall, respectively. These two cases not only represent some of the most common scattering events, but also provide a complete description of all the possible cases. As a matter of fact, a suitable linear combination of these two cases is able to describe any possible surface orientation.

3 Scattering Matrix under Kirchhoff Approximation (KA)

In this Section, we aim at deriving a compact and general expression for the *local* scattering matrix under the framework of Kirchhoff approximation. We show that, after a suitable definition of variables and algebraic manipulations, it is possible to recast the expression of $\underline{\underline{\tilde{S}}}$ in a more convenient form. In particular — and differently from classical approaches [*Tsang and Kong*, 2001; *Ulaby et al.*, 1982; *Barrick*, 1970] — we express the local scattering coefficients in terms of unit wavevectors and surface orientation. This formalism will be exploited for evaluating the scattering coefficients $\tilde{S}_{pq}$, under the KA-GO (see Section 4) and the KA-PO approximations (see Section 5), as well as under the BS configuration (see Section 6).

3.1 Mathematical Derivation

Starting from (7) with the definitions in (5a)–(5b), simple dyadic algebra yields the more compact expression for $\tilde{S}_{pq}$

$$\tilde{S}_{pq} = \underline{F}_p \cdot \hat{e}_{\mathrm{s}q}, \tag{18}$$

where $\underline{F}_p = \underline{F}(\hat{k}_\mathrm{i}, \hat{e}_{\mathrm{i}p}, \hat{n}(\underline{r}'))$. Note that from now on the dependence of $\tilde{S}_{pq}$ on $\hat{k}_\mathrm{i}$, $\hat{k}_\mathrm{s}$, $\hat{n}$, and $\underline{r}'$ is understood, and omitted for clarity purposes. It is worth mentioning here that the use of (18) along with (3) leads to the same results reported in [*Jin and Lax*, 1990; *Elfouhaily et al.*, 2004]. At this stage, since (18) reveals that the knowledge of $\tilde{S}_{pq}$ requires the evaluation of $\underline{F}_p$, it is useful to recast (3) as the sum of three terms

$$\underline{F}_p = \underline{F}_p^0 + \underline{F}_p^\perp + \underline{F}_p^{/\!/}, \tag{19}$$

with

$$\begin{aligned}
\underline{F}_p^0 &= +(\hat{e}_{\mathrm{i}p}\cdot\hat{q}_\mathrm{i})[\hat{k}_\mathrm{s}\times(\hat{n}\times\hat{q}_\mathrm{i}) - (\hat{n}\cdot\hat{k}_\mathrm{i})\hat{q}_\mathrm{i}] + (\hat{e}_{\mathrm{i}p}\cdot\hat{p}_\mathrm{i})[\hat{n}\times\hat{q}_\mathrm{i} + (\hat{n}\cdot\hat{k}_\mathrm{i})(\hat{k}_\mathrm{s}\times\hat{q}_\mathrm{i})],\\
\underline{F}_p^\perp &= +(\hat{e}_{\mathrm{i}p}\cdot\hat{q}_\mathrm{i})[\hat{k}_\mathrm{s}\times(\hat{n}\times\hat{q}_\mathrm{i}) + (\hat{n}\cdot\hat{k}_\mathrm{i})\hat{q}_\mathrm{i}]R_\perp,\\
\underline{F}_p^{/\!/} &= +(\hat{e}_{\mathrm{i}p}\cdot\hat{p}_\mathrm{i})[\hat{n}\times\hat{q}_\mathrm{i} - (\hat{n}\cdot\hat{k}_\mathrm{i})(\hat{k}_\mathrm{s}\times\hat{q}_\mathrm{i})]R_{/\!/},
\end{aligned} \tag{20}$$

being $\underline{F}_p^0$ independent from the Fresnel coefficients, whereas $\underline{F}_p^\perp$ and $\underline{F}_p^{/\!/}$ are related to the perpendicular and parallel Fresnel coefficients, respectively [*Klein and Swift*, 1977; *Franco et al.*, 2017; *Lee and Pottier*, 2009; *Harrington*, 1961, 1993].

At this point, it is convenient to define the following scalar quantities

$$P_p^\mathrm{i} = (\hat{e}_{\mathrm{i}p}\cdot\hat{p}_\mathrm{i}), \tag{21a}$$

$$Q_p^\mathrm{i} = (\hat{e}_{\mathrm{i}p}\cdot\hat{q}_\mathrm{i}), \tag{21b}$$

and vector quantities

$$\begin{aligned}
\underline{t}_\mathrm{i} &= (\hat{n}\times\hat{q}_\mathrm{i}),\\
\underline{t}_\mathrm{s} &= \hat{k}_\mathrm{s}\times(\hat{n}\times\hat{q}_\mathrm{i}),\\
\underline{u}_\mathrm{i} &= (\hat{n}\cdot\hat{k}_\mathrm{i})\hat{q}_\mathrm{i},\\
\underline{u}_\mathrm{s} &= (\hat{n}\cdot\hat{k}_\mathrm{i})(\hat{k}_\mathrm{s}\times\hat{q}_\mathrm{i}),
\end{aligned} \tag{22}$$

so that (20) can be expressed in a more compact form

$$\begin{aligned}\underline{F}_p^0 &= Q_p^{\mathrm{i}}(\underline{t}_{\mathrm{s}} - \underline{u}_{\mathrm{i}}) + P_p^{\mathrm{i}}(\underline{t}_{\mathrm{i}} + \underline{u}_{\mathrm{s}}),\\ \underline{F}_p^{\perp} &= Q_p^{\mathrm{i}}(\underline{t}_{\mathrm{s}} + \underline{u}_{\mathrm{i}})R_{\perp},\\ \underline{F}_p^{/\!/} &= P_p^{\mathrm{i}}(\underline{t}_{\mathrm{i}} - \underline{u}_{\mathrm{s}})R_{/\!/}.\end{aligned} \tag{23}$$

From the definitions in (18) and (19), it follows that even $\tilde{S}_{pq}$ can be expressed as the sum of three terms

$$\tilde{S}_{pq} = \tilde{S}_{pq}^0 + \tilde{S}_{pq}^{\perp} + \tilde{S}_{pq}^{/\!/}, \tag{24}$$

with $\tilde{S}_{pq}^l = \underline{F}_p^l \cdot \hat{e}_{\mathrm{s}q}$ for $l \in \{0,\mathrm{h},\mathrm{v}\}$, so that $\tilde{S}_{pq}$ take the following form:

$$\begin{aligned}\tilde{S}_{pq}^0 &= Q_p^{\mathrm{i}}(\underline{t}_{\mathrm{s}} - \underline{u}_{\mathrm{i}}) \cdot \hat{e}_{\mathrm{s}q} + P_p^{\mathrm{i}}(\underline{t}_{\mathrm{i}} - \underline{u}_{\mathrm{s}}) \cdot \hat{e}_{\mathrm{s}q},\\ \tilde{S}_{pq}^{\perp} &= Q_p^{\mathrm{i}}(\underline{t}_{\mathrm{s}} + \underline{u}_{\mathrm{i}}) \cdot \hat{e}_{\mathrm{s}q} R_{\perp},\\ \tilde{S}_{pq}^{/\!/} &= P_p^{\mathrm{i}}(\underline{t}_{\mathrm{i}} - \underline{u}_{\mathrm{s}}) \cdot \hat{e}_{\mathrm{s}q} R_{/\!/}.\end{aligned} \tag{25}$$

3.2 Scattering Matrix Symmetries

In spite of its compactness and generality, the expression of $\tilde{S}_{pq}$ provided in (25) does not allow for a straightforward calculation of the coefficients since it involves the calculation of different variables that depend on $\hat{k}_{\mathrm{i}}$, $\hat{k}_{\mathrm{s}}$, and $\hat{n}$. However, we show here that, by means of suitable definitions, it is possible to highlight several interesting properties of symmetry, thus considerably reducing the computation of the $\tilde{S}_{pq}$ coefficients.

As a first step, we note that from the definitions (4), (5a) and (21a)–(21b), it is manifest that

$$P_{\mathrm{h}}^{\mathrm{i}} = -Q_{\mathrm{v}}^{\mathrm{i}}, \tag{26a}$$

$$Q_{\mathrm{h}}^{\mathrm{i}} = P_{\mathrm{v}}^{\mathrm{i}}. \tag{26b}$$

Therefore, there is no need to calculate all the four coefficients of $\tilde{S}_{pq}$, since $\tilde{S}_{\mathrm{v}q}$ can be retrieved from $\tilde{S}_{\mathrm{h}q}$ (and vice versa) by exploiting the following relation

$$p : \mathrm{h} \to \mathrm{v} \Rightarrow \begin{cases} P_{\mathrm{h}}^{\mathrm{i}} \to Q_{\mathrm{h}}^{\mathrm{i}} \\ Q_{\mathrm{h}}^{\mathrm{i}} \to -P_{\mathrm{h}}^{\mathrm{i}} \end{cases} \tag{27}$$

thus halving the complexity of the theoretical derivation.

Another interesting symmetry emerges, if one defines the following scalar quantities

$$P_q^{\mathrm{s}} = \hat{e}_{\mathrm{s}q} \cdot (\hat{n} \times \hat{q}_{\mathrm{i}}), \tag{28a}$$

$$Q_q^{\mathrm{s}} = (\hat{e}_{\mathrm{s}q} \cdot \hat{q}_{\mathrm{i}})(\hat{n} \cdot \hat{k}_{\mathrm{i}}), \tag{28b}$$

which in turn allows for defining

$$P_{\pm}^{\mathrm{s}} = (\underline{t}_{\mathrm{i}} \pm \underline{u}_{\mathrm{s}}) \cdot \hat{e}_{\mathrm{sh}} = P_{\mathrm{h}}^{\mathrm{s}} \pm Q_{\mathrm{v}}^{\mathrm{s}}, \tag{29a}$$

$$Q_{\pm}^{\mathrm{s}} = (\underline{t}_{\mathrm{s}} \pm \underline{u}_{\mathrm{i}}) \cdot \hat{e}_{\mathrm{sh}} = P_{\mathrm{v}}^{\mathrm{s}} \pm Q_{\mathrm{h}}^{\mathrm{s}}. \tag{29b}$$

At this point, simple algebra shows that (recall that $\hat{e}_{\mathrm{sv}} = \hat{e}_{\mathrm{sh}} \times \hat{k}_{\mathrm{s}}$ and note that $\underline{t}_{\mathrm{s}} = \hat{k}_{\mathrm{s}} \times \underline{t}_{\mathrm{i}}$ and $\underline{u}_{\mathrm{s}} = \hat{k}_{\mathrm{s}} \times \underline{u}_{\mathrm{i}}$)

$$(\underline{t}_{\mathrm{s}} \pm \underline{u}_{\mathrm{i}}) \cdot \hat{e}_{\mathrm{sv}} = -P_{\mp}^{\mathrm{s}}, \tag{30a}$$

$$(\underline{t}_{\mathrm{i}} \pm \underline{u}_{\mathrm{s}}) \cdot \hat{e}_{\mathrm{sv}} = Q_{\mp}^{\mathrm{s}}. \tag{30b}$$

Therefore, there is no need to calculate both coefficients of $\tilde{S}_{\mathrm{ph}}$ and $\tilde{S}_{\mathrm{pv}}$ since $\tilde{S}_{\mathrm{pv}}$ can be retrieved from $\tilde{S}_{\mathrm{ph}}$ (and vice versa) by exploiting the following relation

$$q : \mathrm{h} \to \mathrm{v} \Rightarrow \begin{cases} P_{\pm}^{\mathrm{s}} \to Q_{\mp}^{\mathrm{s}} \\ Q_{\pm}^{\mathrm{s}} \to -P_{\mp}^{\mathrm{s}} \end{cases} \tag{31}$$

thus halving once again the complexity of the theoretical derivation.

3.3 Analytical expressions

Upon substitution of the definitions (21a)–(21b) and (30a)–(30b) in (25) and the use of symmetries (27) and (31), the scattering matrix $\tilde{S}_{pq}$ takes the following form:

$$\begin{aligned}
\tilde{S}_{\mathrm{hh}} &= +Q^{\mathrm{i}}_{\mathrm{h}}Q^{\mathrm{s}}_{-} + P^{\mathrm{i}}_{\mathrm{h}}P^{\mathrm{s}}_{+} + Q^{\mathrm{i}}_{\mathrm{h}}Q^{\mathrm{s}}_{+}R_{\perp} + P^{\mathrm{i}}_{\mathrm{h}}P^{\mathrm{s}}_{-}R_{/\!/},\\
\tilde{S}_{\mathrm{vh}} &= -P^{\mathrm{i}}_{\mathrm{h}}Q^{\mathrm{s}}_{-} + Q^{\mathrm{i}}_{\mathrm{h}}P^{\mathrm{s}}_{+} - P^{\mathrm{i}}_{\mathrm{h}}Q^{\mathrm{s}}_{+}R_{\perp} + Q^{\mathrm{i}}_{\mathrm{h}}P^{\mathrm{s}}_{-}R_{/\!/},\\
\tilde{S}_{\mathrm{hv}} &= -Q^{\mathrm{i}}_{\mathrm{h}}P^{\mathrm{s}}_{+} + P^{\mathrm{i}}_{\mathrm{h}}Q^{\mathrm{s}}_{-} - Q^{\mathrm{i}}_{\mathrm{h}}P^{\mathrm{s}}_{-}R_{\perp} + P^{\mathrm{i}}_{\mathrm{h}}Q^{\mathrm{s}}_{+}R_{/\!/},\\
\tilde{S}_{\mathrm{vv}} &= +P^{\mathrm{i}}_{\mathrm{h}}P^{\mathrm{s}}_{+} + Q^{\mathrm{i}}_{\mathrm{h}}Q^{\mathrm{s}}_{-} + P^{\mathrm{i}}_{\mathrm{h}}P^{\mathrm{s}}_{-}R_{\perp} + Q^{\mathrm{i}}_{\mathrm{h}}Q^{\mathrm{s}}_{+}R_{/\!/},
\end{aligned} \tag{32}$$

where the $P^{\mathrm{i}}_{\mathrm{h}}$, $Q^{\mathrm{i}}_{\mathrm{h}}$, $P^{\mathrm{s}}_{\pm}$ and $Q^{\mathrm{s}}_{\pm}$ can be made explicit in terms of the incident and scattered wavevectors, i.e., $\hat{k}_{\mathrm{i}}$ and $\hat{k}_{\mathrm{s}}$, and the surface orientation $\hat{n}$:

$$\begin{aligned}
P^{\mathrm{i}}_{\mathrm{h}} &= -\frac{\hat{z}\cdot(\hat{k}_{\mathrm{i}}\times\hat{n})}{|\hat{k}_{\mathrm{i}}\times\hat{z}||\hat{k}_{\mathrm{i}}\times\hat{n}|},\\
Q^{\mathrm{i}}_{\mathrm{h}} &= \frac{(\hat{n}\cdot\hat{z}) - (\hat{k}_{\mathrm{i}}\cdot\hat{n})(\hat{k}_{\mathrm{i}}\cdot\hat{z})}{|\hat{k}_{\mathrm{i}}\times\hat{z}||\hat{k}_{\mathrm{i}}\times\hat{n}|},\\
P^{\mathrm{s}}_{\pm} &= \frac{\hat{z}\cdot(\hat{k}_{\mathrm{i}}\times\hat{n})[(\hat{k}_{\mathrm{s}}\cdot\hat{n}) \pm (\hat{k}_{\mathrm{i}}\cdot\hat{n})]}{|\hat{k}_{\mathrm{s}}\times\hat{z}||\hat{k}_{\mathrm{i}}\times\hat{n}|} + \frac{\hat{k}_{\mathrm{i}}\cdot(\hat{k}_{\mathrm{s}}\times\hat{n})[(\hat{n}\cdot\hat{z}) \pm (\hat{k}_{\mathrm{i}}\cdot\hat{n})(\hat{k}_{\mathrm{s}}\cdot\hat{z})]}{|\hat{k}_{\mathrm{s}}\times\hat{z}||\hat{k}_{\mathrm{i}}\times\hat{n}|},\\
Q^{\mathrm{s}}_{\pm} &= \frac{[(\hat{k}_{\mathrm{s}}\cdot\hat{n}) \mp (\hat{k}_{\mathrm{i}}\cdot\hat{n})][(\hat{k}_{\mathrm{i}}\cdot\hat{z})(\hat{k}_{\mathrm{s}}\cdot\hat{n}) - (\hat{n}\cdot\hat{z})(\hat{k}_{\mathrm{i}}\cdot\hat{k}_{\mathrm{s}})]}{|\hat{k}_{\mathrm{s}}\times\hat{z}||\hat{k}_{\mathrm{i}}\times\hat{n}|} + \frac{[\hat{k}_{\mathrm{i}}\cdot(\hat{k}_{\mathrm{s}}\times\hat{n})][\hat{z}\cdot(\hat{k}_{\mathrm{s}}\times\hat{n})]}{|\hat{k}_{\mathrm{s}}\times\hat{z}||\hat{k}_{\mathrm{i}}\times\hat{n}|}.
\end{aligned} \tag{33}$$

Equation (32) with definitions in (33) furnishes the sought compact and general formalism for evaluating the *local* scattering coefficients under KA as a function of the surface orientation and the incident and scattered wavevectors.

Also, according to the coordinate reference frame depicted in Fig. 1, $\hat{k}_{\mathrm{i}}$, $\hat{k}_{\mathrm{s}}$, and $\hat{n}$ can be expressed as:

$$\begin{aligned}
\hat{k}_{\mathrm{i}} &= \hat{x}\sin\theta_{\mathrm{i}}\cos\phi_{\mathrm{i}} + \hat{y}\sin\theta_{\mathrm{i}}\sin\phi_{\mathrm{i}} + \hat{z}\cos\theta_{\mathrm{i}},\\
\hat{k}_{\mathrm{s}} &= \hat{x}\sin\theta_{\mathrm{s}}\cos\phi_{\mathrm{s}} + \hat{y}\sin\theta_{\mathrm{s}}\sin\phi_{\mathrm{s}} + \hat{z}\cos\theta_{\mathrm{s}},\\
\hat{n} &= \hat{x}\sin\theta_{\mathrm{n}}\cos\phi_{\mathrm{n}} + \hat{y}\sin\theta_{\mathrm{n}}\sin\phi_{\mathrm{n}} + \hat{z}\cos\theta_{\mathrm{n}},
\end{aligned} \tag{34}$$

where $\theta_k \in [0,\pi]$ and $\phi_k \in [-\pi,\pi)$ for $k \in \{\mathrm{i},\mathrm{s},\mathrm{n}\}$. Hence, (32), (33), and (34) completely describe the local scattering matrix, provided that the geometry of acquisition is known. It is worth mentioning here that, to the best of the authors' knowledge, the general form of (32) and (33) has never been reported in the available literature, which only deals with certain specific cases [*Jin and Lax*, 1990; *Elfouhaily et al.*, 2004], taking advantage of the KA-GO approximation.

Interestingly, we should note from (32) that the *local* scattering coefficients satisfy the following symmetries with respect to the Fresnel coefficients

$$\begin{aligned}
\tilde{S}_{\mathrm{vv}}(R_{\perp},R_{/\!/}) &= \tilde{S}_{\mathrm{hh}}(R_{/\!/},R_{\perp}),\\
\tilde{S}_{\mathrm{hv}}(R_{\perp},R_{/\!/}) &= -\tilde{S}_{\mathrm{vh}}(R_{/\!/},R_{\perp}),
\end{aligned} \tag{35}$$

as can be expected from duality and reciprocity principles [*Elfouhaily et al.*, 2004; *Harrington*, 1961]. (Note that $\tilde{S}^0_{\mathrm{vv}} = \tilde{S}^0_{\mathrm{hh}}$ and $\tilde{S}^0_{\mathrm{hv}} = -\tilde{S}^0_{\mathrm{vh}}$.) Furthermore, it is clearly seen that, as a consequence of symmetries (27) and (31), the scattering coefficients also possess the following symmetries with respect to the definitions of $P^{\mathrm{i}}_{\mathrm{h}}$, $Q^{\mathrm{i}}_{\mathrm{h}}$, $P^{\mathrm{s}}_{\pm}$ and $Q^{\mathrm{s}}_{\pm}$

$$\begin{aligned}
\tilde{S}_{\mathrm{vh}}(P^{\mathrm{i}}_{\mathrm{h}},Q^{\mathrm{i}}_{\mathrm{h}},P^{\mathrm{s}}_{\pm},Q^{\mathrm{s}}_{\pm}) &= \tilde{S}_{\mathrm{hh}}(Q^{\mathrm{i}}_{\mathrm{h}},-P^{\mathrm{i}}_{\mathrm{h}},P^{\mathrm{s}}_{\pm},Q^{\mathrm{s}}_{\pm}),\\
\tilde{S}_{\mathrm{hv}}(P^{\mathrm{i}}_{\mathrm{h}},Q^{\mathrm{i}}_{\mathrm{h}},P^{\mathrm{s}}_{\pm},Q^{\mathrm{s}}_{\pm}) &= \tilde{S}_{\mathrm{hh}}(P^{\mathrm{i}}_{\mathrm{h}},Q^{\mathrm{i}}_{\mathrm{h}},Q^{\mathrm{s}}_{\mp},-P^{\mathrm{s}}_{\mp}),\\
\tilde{S}_{\mathrm{vv}}(P^{\mathrm{i}}_{\mathrm{h}},Q^{\mathrm{i}}_{\mathrm{h}},P^{\mathrm{s}}_{\pm},Q^{\mathrm{s}}_{\pm}) &= \tilde{S}_{\mathrm{hh}}(Q^{\mathrm{i}}_{\mathrm{h}},-P^{\mathrm{i}}_{\mathrm{h}},Q^{\mathrm{s}}_{\mp},-P^{\mathrm{s}}_{\mp}).
\end{aligned} \tag{36}$$

As a final remark, we should note that, although the calculation of a single scattering coefficient suffices for determining the remaining ones, their expressions will always be reported for the sake of completeness. Indeed, it should be stressed that the four scattering coefficients are independent of one another, hence one cannot generally retrieve the other coefficients from a single direct measurement. In this light, it is clear that once the Fresnel coefficients and the quantities in (33) are known, one can evaluate any of the scattering coefficients in (32), and easily retrieve the remaining three by means of (35) and (36). This will considerably simplify the analytical derivation of the scattering coefficients under KA-GO and KA-PO approximations, as we will see in the next Sections 4 and 5, respectively.

4 Scattering Matrix under KA-GO Approximation

As has been shown in Subsection 2.1, under KA-GO approximation the *local* scattering matrix $\tilde{S}_{pq}$ coincides with the scattering matrix S_{pq}. Without loss of generality, analytical expressions are here reported for the scattering matrix.

Using the relations (15a)–(15d), the scattering matrix can be considerably simplified. Indeed, it is easily seen that $P^{\mathrm{s}}_{+}=0$ and $Q^{\mathrm{s}}_{-}=0$, thus

$$\begin{aligned}
S_{\mathrm{hh}} &= +Q^{\mathrm{i}}_{\mathrm{h}}Q^{\mathrm{s}}_{+}R_{\perp}+P^{\mathrm{i}}_{\mathrm{h}}P^{\mathrm{s}}_{-}R_{/\!/},\\
S_{\mathrm{vh}} &= -P^{\mathrm{i}}_{\mathrm{h}}Q^{\mathrm{s}}_{+}R_{\perp}+Q^{\mathrm{i}}_{\mathrm{h}}P^{\mathrm{s}}_{-}R_{/\!/},\\
S_{\mathrm{hv}} &= -Q^{\mathrm{i}}_{\mathrm{h}}P^{\mathrm{s}}_{-}R_{\perp}+P^{\mathrm{i}}_{\mathrm{h}}Q^{\mathrm{s}}_{+}R_{/\!/},\\
S_{\mathrm{vv}} &= +P^{\mathrm{i}}_{\mathrm{h}}P^{\mathrm{s}}_{-}R_{\perp}+Q^{\mathrm{i}}_{\mathrm{h}}Q^{\mathrm{s}}_{+}R_{/\!/},
\end{aligned} \tag{37}$$

with

$$\begin{aligned}
P^{\mathrm{i}}_{\mathrm{h}} &= \frac{-\hat{z}\cdot(\hat{k}_{\mathrm{i}}\times\hat{k}_{\mathrm{s}})}{2(\hat{k}_{\mathrm{s}}\cdot\hat{n})|\hat{k}_{\mathrm{i}}\times\hat{z}||\hat{k}_{\mathrm{i}}\times\hat{n}|},\\
Q^{\mathrm{i}}_{\mathrm{h}} &= \frac{[(\hat{k}_{\mathrm{s}}\cdot\hat{z})-(\hat{k}_{\mathrm{i}}\cdot\hat{z})]+2(\hat{k}_{\mathrm{i}}\cdot\hat{z})(\hat{k}_{\mathrm{s}}\cdot\hat{n})^2}{2(\hat{k}_{\mathrm{s}}\cdot\hat{n})|\hat{k}_{\mathrm{i}}\times\hat{z}||\hat{k}_{\mathrm{i}}\times\hat{n}|},\\
P^{\mathrm{s}}_{-} &= \frac{\hat{z}\cdot(\hat{k}_{\mathrm{i}}\times\hat{k}_{\mathrm{s}})}{|\hat{k}_{\mathrm{s}}\times\hat{z}||\hat{k}_{\mathrm{i}}\times\hat{n}|},\\
Q^{\mathrm{s}}_{+} &= \frac{2(\hat{k}_{\mathrm{i}}\cdot\hat{z})(\hat{k}_{\mathrm{s}}\cdot\hat{n})^2-(\hat{k}_{\mathrm{s}}\cdot\hat{k}_{\mathrm{i}})[(\hat{k}_{\mathrm{s}}\cdot\hat{z})-(\hat{k}_{\mathrm{i}}\cdot\hat{z})]}{|\hat{k}_{\mathrm{s}}\times\hat{z}||\hat{k}_{\mathrm{i}}\times\hat{n}|}.
\end{aligned} \tag{38}$$

We note here that by replacing the definitions of P^{i}_{p}, Q^{i}_{p} for $\mathrm{p}\in\{\mathrm{h},\mathrm{v}\}$ and $P^{\mathrm{s}}_{\pm}$, $Q^{\mathrm{s}}_{\pm}$ as in (21a)-(21b) and (29a)-(29b), respectively, in (37), it is possible (after suitable algebraic manipulations) to obtain the results reported in [*Stogryn*, 1967] (see Eqs. (52a)-(52d)), and in compact dyadic form in [*Jin and Lax*, 1990; *Elfouhaily et al.*, 2004] (see Eqs. (10a)-(10b), and (E.10), respectively).

Even more interestingly, these expressions can also be given in terms of angles through (34). Moreover, under KA-GO $\hat{k}_{\mathrm{i}}$, $\hat{k}_{\mathrm{s}}$, and $\hat{n}$ are related through the specular point condition (13). Hence, the scattering matrix can be expressed in terms of the sole incident and scattered angles, i.e., θ_{i}, ϕ_{i}, and θ_{s}, ϕ_{s}, respectively. As a matter of fact, for deterministic surfaces $\hat{k}_{\mathrm{s}}$ is given by (13), and θ_{s}, ϕ_{s} can unambiguously be retrieved through the relations

$$\begin{aligned}
\theta_{\mathrm{s}} &= \arccos(\hat{k}_{\mathrm{s}}\cdot\hat{z}),\\
\phi_{\mathrm{s}} &= \arctan 2[(\hat{k}_{\mathrm{s}}\cdot\hat{y}),(\hat{k}_{\mathrm{s}}\cdot\hat{x})],
\end{aligned} \tag{39}$$

where arctan2(·,·) is the multi-valued inverse tangent function. The final expressions for the scattering coefficients are therefore:

$$\begin{aligned}
S_{\mathrm{hh}} =& +S_0\{+R_\perp(\psi)[\sin\theta_\mathrm{i}\cos\theta_\mathrm{s}-\cos\theta_\mathrm{i}\sin\theta_\mathrm{s}\cos(\phi_\mathrm{i}-\phi_\mathrm{s})][\cos\theta_\mathrm{i}\sin\theta_\mathrm{s}-\sin\theta_\mathrm{i}\cos\theta_\mathrm{s}\cos(\phi_\mathrm{i}-\phi_\mathrm{s})]\\
&-R_{/\!/}(\psi)\sin\theta_\mathrm{i}\sin\theta_\mathrm{s}\sin^2(\phi_\mathrm{i}-\phi_\mathrm{s})\},\\
S_{\mathrm{vh}} =& -S_0\{R_\perp(\psi)[\sin\theta_\mathrm{s}\sin(\phi_\mathrm{i}-\phi_\mathrm{s})][\cos\theta_\mathrm{i}\sin\theta_\mathrm{s}-\sin\theta_\mathrm{i}\cos\theta_\mathrm{s}\cos(\phi_\mathrm{i}-\phi_\mathrm{s})]\\
&+R_{/\!/}(\psi)[\sin\theta_\mathrm{i}\sin(\phi_\mathrm{i}-\phi_\mathrm{s})][\sin\theta_\mathrm{i}\cos\theta_\mathrm{s}-\cos\theta_\mathrm{i}\sin\theta_\mathrm{s}\cos(\phi_\mathrm{i}-\phi_\mathrm{s})]\},\\
S_{\mathrm{hv}} =& +S_0\{R_\perp(\psi)[\sin\theta_\mathrm{i}\sin(\phi_\mathrm{i}-\phi_\mathrm{s})][\sin\theta_\mathrm{i}\cos\theta_\mathrm{s}-\cos\theta_\mathrm{i}\sin\theta_\mathrm{s}\cos(\phi_\mathrm{i}-\phi_\mathrm{s})]\\
&+R_{/\!/}(\psi)[\sin\theta_\mathrm{s}\sin(\phi_\mathrm{i}-\phi_\mathrm{s})][\cos\theta_\mathrm{i}\sin\theta_\mathrm{s}-\sin\theta_\mathrm{i}\cos\theta_\mathrm{s}\cos(\phi_\mathrm{i}-\phi_\mathrm{s})]\},\\
S_{\mathrm{vv}} =& +S_0\{-R_\perp(\psi)\sin\theta_\mathrm{i}\sin\theta_\mathrm{s}\sin^2(\phi_\mathrm{i}-\phi_\mathrm{s})\\
&+R_{/\!/}(\psi)[\sin\theta_\mathrm{i}\cos\theta_\mathrm{s}-\cos\theta_\mathrm{i}\sin\theta_\mathrm{s}\cos(\phi_\mathrm{i}-\phi_\mathrm{s})][\cos\theta_\mathrm{i}\sin\theta_\mathrm{s}-\sin\theta_\mathrm{i}\cos\theta_\mathrm{s}\cos(\phi_\mathrm{i}-\phi_\mathrm{s})]\},
\end{aligned} \tag{40}$$

having defined $S_0 = 1/(2\cos\psi\sin^2\psi)$ where ψ can also be expressed in terms of the incident and scattered angles as:

$$\psi = \arccos\sqrt{\frac{1-\sin\theta_\mathrm{i}\sin\theta_\mathrm{s}\cos(\phi_\mathrm{i}-\phi_\mathrm{s})-\cos\theta_\mathrm{i}\cos\theta_\mathrm{s}}{2}}. \tag{41}$$

Results are in agreement with those reported in [*Ulaby et al.*, 1982]. Note that the dependence of the Fresnel coefficients on ψ has been explicited in (40), and this would be the case for all final expressions.

5 Scattering Matrix under KA-PO Approximation

As emphasized in the previous Section 3, KA and KA-PO coincides when considering scattering from a plane. The same result holds for rough surfaces, provided that the $\hat{n}_0$ describes the normal unit vector of the mean plane. In these cases, as for KA-GO, the *local* scattering matrix $\tilde{S}_{pq}$ coincides with the scattering matrix S_{pq}. As a result, expressions for the scattering matrix are still given by (32) and (33) upon the substitution $\hat{n}(r') = \hat{n}_0$.

However, some further simplifications are possible when considering the relevant cases of $\hat{n}\cdot\hat{z} = 0$ (Subsection 5.1) and $\hat{n} = \hat{z}$ (Subsection 5.2), corresponding to the cases of scattering from a wall and scattering from ground, respectively.

5.1 Specific case: $\hat{n}\cdot\hat{z} = 0$

As is manifest from (33), the quantities Q^i_h, $P^\mathrm{s}_\pm$, and $Q^\mathrm{s}_\pm$ all contain terms that depend on $\hat{n}\cdot\hat{z}$, thus the hypothesis $\hat{n}\cdot\hat{z} = 0$ allows for simplifying their expressions as follows:

$$\begin{aligned}
P^\mathrm{i}_\mathrm{h} =& -\frac{\hat{z}\cdot(\hat{k}_\mathrm{i}\times\hat{n})}{|\hat{k}_\mathrm{i}\times\hat{z}||\hat{k}_\mathrm{i}\times\hat{n}|},\\
Q^\mathrm{i}_\mathrm{h} =& \frac{-(\hat{k}_\mathrm{i}\cdot\hat{n})(\hat{k}_\mathrm{i}\cdot\hat{z})}{|\hat{k}_\mathrm{i}\times\hat{z}||\hat{k}_\mathrm{i}\times\hat{n}|},\\
P^\mathrm{s}_\pm =& \frac{[(\hat{k}_\mathrm{s}\cdot\hat{n})\pm(\hat{k}_\mathrm{i}\cdot\hat{n})][\hat{z}\cdot(\hat{k}_\mathrm{i}\times\hat{n})]}{|\hat{k}_\mathrm{s}\times\hat{z}||\hat{k}_\mathrm{i}\times\hat{n}|} \pm \frac{[\hat{k}_\mathrm{i}\cdot(\hat{k}_\mathrm{s}\times\hat{n})][(\hat{k}_\mathrm{i}\cdot\hat{n})(\hat{k}_\mathrm{s}\cdot\hat{z})]}{|\hat{k}_\mathrm{s}\times\hat{z}||\hat{k}_\mathrm{i}\times\hat{n}|},\\
Q^\mathrm{s}_\pm =& \frac{[(\hat{k}_\mathrm{s}\cdot\hat{n})\mp(\hat{k}_\mathrm{i}\cdot\hat{n})][(\hat{k}_\mathrm{i}\cdot\hat{z})(\hat{k}_\mathrm{s}\cdot\hat{n})]}{|\hat{k}_\mathrm{s}\times\hat{z}||\hat{k}_\mathrm{i}\times\hat{n}|} + \frac{[\hat{k}_\mathrm{i}\cdot(\hat{k}_\mathrm{s}\times\hat{n})][\hat{z}\cdot(\hat{k}_\mathrm{s}\times\hat{n})]}{|\hat{k}_\mathrm{s}\times\hat{z}||\hat{k}_\mathrm{i}\times\hat{n}|}.
\end{aligned} \tag{42}$$

Hence, (32) with (42) constitute the simplified set of equations to be used under KA-PO approximation. As has already been done for KA-GO, it is also useful to provide explicit analytical expressions in terms of angles. However, different from the KA-GO approximation, the surface aspect angle ϕ_n is needed (being $\theta_\mathrm{n} = \pi/2$). Thus, final expressions are

given in terms of the five angles, i.e., θ_i, ϕ_i, θ_s, ϕ_s, and ϕ_n. After lenghty calculations, the scattering coefficients are found to be equal to:

$$\begin{aligned}
S_\mathrm{hh} = &+T_0\{[1-\sin^2\theta_\mathrm{i}\cos^2(\phi_\mathrm{i}-\phi_\mathrm{n})][\sin\theta_\mathrm{s}\cos(\phi_\mathrm{i}-\phi_\mathrm{n})+\sin\theta_\mathrm{i}\cos(\phi_\mathrm{s}-\phi_\mathrm{n})]\\
&+R_\perp(\psi)[\cos^2\theta_\mathrm{i}\sin\theta_\mathrm{s}\cos(\phi_\mathrm{i}-\phi_\mathrm{n})\\
&-\cos\theta_\mathrm{i}\sin\theta_\mathrm{i}\cos\theta_\mathrm{s}\cos(\phi_\mathrm{i}-\phi_\mathrm{n})\sin(\phi_\mathrm{i}-\phi_\mathrm{n})\sin(\phi_\mathrm{s}-\phi_\mathrm{n})\\
&-\cos^2\theta_\mathrm{i}\sin\theta_\mathrm{i}\cos^2(\phi_\mathrm{i}-\phi_\mathrm{n})\cos(\phi_\mathrm{s}-\phi_\mathrm{n})]\\
&+R_{/\!/}(\psi)[\sin\theta_\mathrm{i}\sin^2(\phi_\mathrm{i}-\phi_\mathrm{n})\cos(\phi_\mathrm{s}-\phi_\mathrm{n})\\
&-\cos\theta_\mathrm{i}\sin\theta_\mathrm{i}\cos\theta_\mathrm{s}\cos(\phi_\mathrm{i}-\phi_\mathrm{n})\sin(\phi_\mathrm{i}-\phi_\mathrm{n})\sin(\phi_\mathrm{s}-\phi_\mathrm{n})\\
&-\sin^2\theta_\mathrm{i}\sin\theta_\mathrm{s}\cos(\phi_\mathrm{i}-\phi_\mathrm{n})\sin^2(\phi_\mathrm{i}-\phi_\mathrm{n})]\},
\end{aligned}$$

$$\begin{aligned}
S_\mathrm{vh} = &+T_0\{[1-\sin^2\theta_\mathrm{i}\cos^2(\phi_\mathrm{i}-\phi_\mathrm{n})][\cos\theta_\mathrm{i}\sin\theta_\mathrm{s}\sin(\phi_\mathrm{i}-\phi_\mathrm{n})-\sin\theta_\mathrm{i}\cos\theta_\mathrm{s}\sin(\phi_\mathrm{s}-\phi_\mathrm{n})]\\
&+R_\perp(\psi)[\cos\theta_\mathrm{i}\sin\theta_\mathrm{s}\sin(\phi_\mathrm{i}-\phi_\mathrm{n})\\
&-\cos\theta_\mathrm{i}\sin\theta_\mathrm{i}\cos(\phi_\mathrm{i}-\phi_\mathrm{n})\sin(\phi_\mathrm{i}-\phi_\mathrm{n})\cos(\phi_\mathrm{s}-\phi_\mathrm{n})\\
&-\sin\theta_\mathrm{i}\cos\theta_\mathrm{s}\sin^2(\phi_\mathrm{i}-\phi_\mathrm{n})\sin(\phi_\mathrm{s}-\phi_\mathrm{n})]\\
&+R_{/\!/}(\psi)[\sin^2\theta_\mathrm{i}\cos\theta_\mathrm{i}\sin\theta_\mathrm{s}\cos^2(\phi_\mathrm{i}-\phi_\mathrm{n})\sin(\phi_\mathrm{i}-\phi_\mathrm{n})\\
&-\cos\theta_\mathrm{i}\sin\theta_\mathrm{i}\cos(\phi_\mathrm{i}-\phi_\mathrm{n})\sin(\phi_\mathrm{i}-\phi_\mathrm{n})\cos(\phi_\mathrm{s}-\phi_\mathrm{n})\\
&+\cos^2\theta_\mathrm{i}\sin\theta_\mathrm{i}\cos\theta_\mathrm{s}\cos^2(\phi_\mathrm{i}-\phi_\mathrm{n})\sin(\phi_\mathrm{s}-\phi_\mathrm{n})]\},
\end{aligned}$$

$$\begin{aligned}
S_\mathrm{hv} = &-T_0\{[1-\sin^2\theta_\mathrm{i}\cos^2(\phi_\mathrm{i}-\phi_\mathrm{n})][\cos\theta_\mathrm{i}\sin\theta_\mathrm{s}\sin(\phi_\mathrm{i}-\phi_\mathrm{n})-\sin\theta_\mathrm{i}\cos\theta_\mathrm{s}\sin(\phi_\mathrm{s}-\phi_\mathrm{n})]\\
&+R_\perp(\psi)[\sin^2\theta_\mathrm{i}\cos\theta_\mathrm{i}\sin\theta_\mathrm{s}\cos^2(\phi_\mathrm{i}-\phi_\mathrm{n})\sin(\phi_\mathrm{i}-\phi_\mathrm{n})\\
&-\cos\theta_\mathrm{i}\sin\theta_\mathrm{i}\cos(\phi_\mathrm{i}-\phi_\mathrm{n})\sin(\phi_\mathrm{i}-\phi_\mathrm{n})\cos(\phi_\mathrm{s}-\phi_\mathrm{n})\\
&+\cos^2\theta_\mathrm{i}\sin\theta_\mathrm{i}\cos\theta_\mathrm{s}\cos^2(\phi_\mathrm{i}-\phi_\mathrm{n})\sin(\phi_\mathrm{s}-\phi_\mathrm{n})]\\
&+R_{/\!/}(\psi)[\cos\theta_\mathrm{i}\sin\theta_\mathrm{s}\sin(\phi_\mathrm{i}-\phi_\mathrm{n})\\
&-\cos\theta_\mathrm{i}\sin\theta_\mathrm{i}\cos(\phi_\mathrm{i}-\phi_\mathrm{n})\sin(\phi_\mathrm{i}-\phi_\mathrm{n})\cos(\phi_\mathrm{s}-\phi_\mathrm{n})\\
&-\sin\theta_\mathrm{i}\cos\theta_\mathrm{s}\sin^2(\phi_\mathrm{i}-\phi_\mathrm{n})\sin(\phi_\mathrm{s}-\phi_\mathrm{n})]\},
\end{aligned}$$

$$\begin{aligned}
S_\mathrm{vv} = &+T_0\{[1-\sin^2\theta_\mathrm{i}\cos^2(\phi_\mathrm{i}-\phi_\mathrm{n})][\sin\theta_\mathrm{s}\cos(\phi_\mathrm{i}-\phi_\mathrm{n})+\sin\theta_\mathrm{i}\cos(\phi_\mathrm{s}-\phi_\mathrm{n})]\\
&+R_\perp(\psi)[\sin\theta_\mathrm{i}\sin^2(\phi_\mathrm{i}-\phi_\mathrm{n})\cos(\phi_\mathrm{s}-\phi_\mathrm{n})\\
&-\cos\theta_\mathrm{i}\sin\theta_\mathrm{i}\cos\theta_\mathrm{s}\cos(\phi_\mathrm{i}-\phi_\mathrm{n})\sin(\phi_\mathrm{i}-\phi_\mathrm{n})\sin(\phi_\mathrm{s}-\phi_\mathrm{n})\\
&-\sin^2\theta_\mathrm{i}\sin\theta_\mathrm{s}\cos(\phi_\mathrm{i}-\phi_\mathrm{n})\sin^2(\phi_\mathrm{i}-\phi_\mathrm{n})]\\
&+R_{/\!/}(\psi)[\cos^2\theta_\mathrm{i}\sin\theta_\mathrm{s}\cos(\phi_\mathrm{i}-\phi_\mathrm{n})\\
&-\cos\theta_\mathrm{i}\sin\theta_\mathrm{i}\cos\theta_\mathrm{s}\cos(\phi_\mathrm{i}-\phi_\mathrm{n})\sin(\phi_\mathrm{i}-\phi_\mathrm{n})\sin(\phi_\mathrm{s}-\phi_\mathrm{n})\\
&-\cos^2\theta_\mathrm{i}\sin\theta_\mathrm{i}\cos^2(\phi_\mathrm{i}-\phi_\mathrm{n})\cos(\phi_\mathrm{s}-\phi_\mathrm{n})]\},
\end{aligned} \tag{43}$$

having defined $T_0 = -1/\sin^2\psi$, whereas ψ can also be expressed in terms of local angles as:

$$\psi = \arccos[-\sin\theta_\mathrm{i}\cos(\phi_\mathrm{i}-\phi_\mathrm{n})]. \tag{44}$$

We should note that the case $\hat{n}\cdot\hat{z}=0$ has never been reported in the available literature.

As a final comment, it is worth noting that, as opposed to KA-GO, the expressions of the scattering coefficients for KA-PO under the case $\hat{n}\cdot\hat{z}=0$ possess the S^0_{pq} term that is present even when the Fresnel coefficients are both zero. This term also appears under the hypothesis $\hat{n}=\hat{z}$, as we will see in the next Subsection 5.2.

5.2 Specific case: $\hat{n}=\hat{z}$

As is clear from the definitions of $\hat{q}_\mathrm{i}$, $\hat{p}_\mathrm{i}$, and $\hat{e}_\mathrm{ih}$, $\hat{e}_\mathrm{iv}$ [see (4), and (5a), respectively], under the hypothesis $\hat{n}=\hat{z}$ we have that $\hat{q}_\mathrm{i}=\hat{e}_\mathrm{ih}$ and $\hat{p}_\mathrm{i}=\hat{e}_\mathrm{iv}$, thus $P^\mathrm{i}_\mathrm{h}=0$ and $Q^\mathrm{i}_\mathrm{h}=1$, and

the scattering matrix takes the following simplified form:

$$\begin{aligned} S_{\rm hh} &= +Q^{\rm s}_{-} + Q^{\rm s}_{+} R_{\perp}, \\ S_{\rm vh} &= +P^{\rm s}_{+} + P^{\rm s}_{-} R_{/\!/}, \\ S_{\rm hv} &= -P^{\rm s}_{-} - P^{\rm s}_{-} R_{\perp}, \\ S_{\rm vv} &= +Q^{\rm s}_{-} + Q^{\rm s}_{+} R_{/\!/}, \end{aligned} \tag{45}$$

with

$$\begin{aligned} P^{\rm s}_{\pm} &= \frac{[\hat{z}\cdot(\hat{k}_{\rm i}\times\hat{k}_{\rm s})][1\pm(\hat{k}_{\rm s}\cdot\hat{z})(\hat{k}_{\rm i}\cdot\hat{z})]}{|\hat{k}_{\rm s}\times\hat{z}||\hat{k}_{\rm i}\times\hat{n}|}, \\ Q^{\rm s}_{\pm} &= \frac{[(\hat{k}_{\rm i}\cdot\hat{z})(\hat{k}_{\rm s}\cdot\hat{z})-(\hat{k}_{\rm s}\cdot\hat{k}_{\rm i})][(\hat{k}_{\rm s}\cdot\hat{z})\mp(\hat{k}_{\rm i}\cdot\hat{z})]}{|\hat{k}_{\rm s}\times\hat{z}||\hat{k}_{\rm i}\times\hat{n}|}. \end{aligned} \tag{46}$$

As for KA-GO approximation, the scattering coefficients no longer depend on the aspect angle $\phi_{\rm n}$, since the surface is oriented exactly along the vertical z-axis. Therefore, the analytical expressions of the scattering coefficients are given in terms of the incident and scattered angles only. After simple algebraic manipulations, the scattering coefficients are found to be equal to:

$$\begin{aligned} S_{\rm hh} &= \cos(\phi_{\rm s}-\phi_{\rm i})[R_{\perp}(\psi)(\cos\theta_{\rm i}-\cos\theta_{\rm s})-\cos\theta_{\rm i}-\cos\theta_{\rm s}], \\ S_{\rm vh} &= \sin(\phi_{\rm s}-\phi_{\rm i})[R_{/\!/}(\psi)(1-\cos\theta_{\rm i}\cos\theta_{\rm s})+1+\cos\theta_{\rm i}\cos\theta_{\rm s}], \\ S_{\rm hv} &= -\sin(\phi_{\rm s}-\phi_{\rm i})[R_{\perp}(\psi)(1-\cos\theta_{\rm i}\cos\theta_{\rm s})+1+\cos\theta_{\rm i}\cos\theta_{\rm s}], \\ S_{\rm vv} &= \cos(\phi_{\rm s}-\phi_{\rm i})[R_{/\!/}(\psi)(\cos\theta_{\rm i}-\cos\theta_{\rm s})-\cos\theta_{\rm i}-\cos\theta_{\rm s}], \end{aligned} \tag{47}$$

where the local incidence angle is simply given by $\psi = \pi - \theta_{\rm i}$. Results are in agreement with those reported in [*Tsang and Kong*, 2001].

6 Backscattering Case

In the previous Sections 4 and 5, we have provided simplified sets of equations for evaluating the scattering matrix under the KA-GO and the KA-PO approximations, respectively. In this Section, we aim at furnishing simplified expressions under the backscattering hypothesis, i.e., $\hat{k}_{\rm s} = -\hat{k}_{\rm i}$. Our interest in analyzing the BS case is not only its extensive use in all monostatic scenarios, but in that it also provides a further method to validate the previous formulas. As a matter of fact, in [*Franceschetti et al.*, 2002] analytical expressions for the scattering matrix under both the KA-GO and the KA-PO approximations were found under the BS case. In Subsection 6.1 we furnish simplified expressions in the backscattering limit, whereas in Subsection 6.2 we show that our general formulas coincide with those provided in [*Franceschetti et al.*, 2002] in the BS case.

6.1 Kirchhoff approximation

In the most general case, under the BS hypothesis the surface orientation is not fixed, thus the *local* scattering matrix has to be used. However, under the BS case, (32) and (33) can be considerably simplified. Indeed, it is easily seen that by letting $\hat{k}_{\rm s} = -\hat{k}_{\rm i}$, it follows that $P^{\rm s}_{+} = 0$ and $Q^{\rm s}_{-} = 0$, whereas $P^{\rm s}_{-} = 2(\hat{k}_{\rm i}\cdot\hat{n})P^{\rm i}_{\rm h}$ and $Q^{\rm s}_{+} = -2(\hat{k}_{\rm i}\cdot\hat{n})Q^{\rm i}_{\rm h}$, so that (32) reads:

$$\begin{aligned} \tilde{S}_{\rm hh} &= -2(\hat{k}_{\rm i}\cdot\hat{n})[(Q^{\rm i}_{\rm h})^2 R_{\perp} - (P^{\rm i}_{\rm h})^2 R_{/\!/}], \\ \tilde{S}_{\rm vh} &= -\tilde{S}_{\rm hv} = +2(\hat{k}_{\rm i}\cdot\hat{n})P^{\rm i}_{\rm h}Q^{\rm i}_{\rm h}[R_{\perp} + R_{/\!/}], \\ \tilde{S}_{\rm vv} &= +2(\hat{k}_{\rm i}\cdot\hat{n})[(P^{\rm i}_{\rm h})^2 R_{\perp} - (Q^{\rm i}_{\rm h})^2 R_{/\!/}], \end{aligned} \tag{48}$$

with

$$P^{\rm i}_{\rm h} = -\frac{\hat{z}\cdot(\hat{k}_{\rm i}\times\hat{n})}{|\hat{k}_{\rm i}\times\hat{z}||\hat{k}_{\rm i}\times\hat{n}|}, \quad Q^{\rm i}_{\rm h} = \frac{(\hat{n}\cdot\hat{z})-(\hat{k}_{\rm i}\cdot\hat{z})(\hat{k}_{\rm i}\cdot\hat{n})}{|\hat{k}_{\rm i}\times\hat{z}||\hat{k}_{\rm i}\times\hat{n}|}. \tag{49}$$

The analytical expressions are given in terms of the incident angles and the surface orientation angles only, i.e., θ_i, ϕ_i, and θ_n, ϕ_n, being $\theta_s = \pi - \theta_\mathrm{i}$, $\phi_\mathrm{s} = \phi_\mathrm{i} + \pi$ in the BS case. Simple algebra leads us to the following expressions:

$$\begin{aligned}
\tilde{S}_\mathrm{hh} &= \frac{2\cos\psi}{\sin^2\psi}\{R_\perp(\psi)[\sin\theta_\mathrm{i}\cos\theta_\mathrm{n} - \cos\theta_\mathrm{i}\sin\theta_\mathrm{n}\cos(\phi_\mathrm{i}-\phi_\mathrm{n})]^2 - R_{/\!/}(\psi)\sin^2\theta_\mathrm{n}\sin^2(\phi_\mathrm{i}-\phi_\mathrm{n})\},\\
\tilde{S}_\mathrm{vh} &= -\tilde{S}_\mathrm{hv} = -\frac{2\cos\psi}{\sin^2\psi}[R_\perp(\psi) + R_{/\!/}(\psi)][\sin\theta_\mathrm{n}\sin(\phi_\mathrm{i}-\phi_\mathrm{n})]\\
&\quad [\sin\theta_\mathrm{i}\cos\theta_\mathrm{n} - \cos\theta_\mathrm{i}\sin\theta_\mathrm{n}\cos(\phi_\mathrm{i}-\phi_\mathrm{n})],\\
\tilde{S}_\mathrm{vv} &= \frac{2\cos\psi}{\sin^2\psi}\{R_{/\!/}(\psi)[\sin\theta_\mathrm{i}\cos\theta_\mathrm{n} - \cos\theta_\mathrm{i}\sin\theta_\mathrm{n}\cos(\phi_\mathrm{i}-\phi_\mathrm{n})]^2 - R_\perp(\psi)\sin^2\theta_\mathrm{n}\sin^2(\phi_\mathrm{i}-\phi_\mathrm{n})\},
\end{aligned} \tag{50}$$

where ψ can also be expressed as:

$$\psi = \arccos[-\sin\theta_\mathrm{i}\sin\theta_\mathrm{n}\cos(\phi_\mathrm{i}-\phi_\mathrm{n}) - \cos\theta_\mathrm{i}\cos\theta_\mathrm{n}]. \tag{51}$$

We should note that, in spite of the wide interest in the backscattering case, general expressions as those in (48), (49) and (50) have never been reported in the available literature.

6.2 Validation of analytical formulas under KA

Here, we aim at validating the scattering coefficients in (50) through the approach proposed in [*Franceschetti et al.*, 2002]. Specifically, the cases of single-bounce contributions from the ground and from a wall under KA-GO and KA-PO approximations are analyzed. We chose the same coordinate reference frame as defined in [*Franceschetti et al.*, 2002], therefore the former case implies $\hat{n} = \hat{z}$, whereas the latter case implies $\hat{n}\cdot\hat{z} = 0$. In addition, it is useful to recover the definitions of the angles θ, ϕ as in [*Franceschetti et al.*, 2002] through the following substitutions:

$$\begin{aligned}
\theta_\mathrm{i} &= \pi - \theta,\\
\phi_\mathrm{i} &= -\pi/2,\\
\phi_\mathrm{n} &= \pi/2 - \phi,
\end{aligned} \tag{52}$$

whereas the relations with the scattered angles follow from the BS hypothesis

$$\begin{aligned}
\theta_\mathrm{s} &= \pi - \theta_\mathrm{i},\\
\phi_\mathrm{s} &= \phi_\mathrm{i} + \pi.
\end{aligned} \tag{53}$$

It is worth mentioning that (52) reveals that (50) generalizes the backscattering formulas found in [*Franceschetti et al.*, 2002] to the case of incidence over an arbitrary azimuthal plane (i.e., any ϕ_i) which could be extremely useful for directly evaluating the (back)scattering matrix when multiple-bounce contributions are considered.

6.2.1 KA-GO

Under KA-GO and BS approximation, we have $\hat{n} = -\hat{k}_\mathrm{i}$, thus

$$\begin{aligned}
\theta_\mathrm{n} &= \theta_\mathrm{s},\\
\phi_\mathrm{n} &= \phi_\mathrm{s}.
\end{aligned} \tag{54}$$

We should comment that, for $\hat{n} = -\hat{k}_\mathrm{i}$, the local orthonormal system [viz., $(\hat{p}_\mathrm{i}, \hat{q}_\mathrm{i}, \hat{k}_\mathrm{i})$] is no longer well-defined (leading to an indeterminate form), and the resulting formulas have to be understood in the asymptotic limit of $\hat{n} \sim -\hat{k}_\mathrm{i}$. As a result, backscattering from the wall is always zero except for the limiting case of $\theta = \pi/2$ and $\phi = 0$, as is seen from either (50) or (40) evaluated at $\theta_\mathrm{n} = \pi/2$, thus confirming the results in [*Franceschetti et al.*, 2002].

With regard to the backscattering from ground, S_{pq} is given either by (50) for $\theta_{\mathrm{n}}=0$, or by (40) for $\theta_{\mathrm{n}}=0$ upon subsitution of (53). Thus, it is easily found that

$$\begin{aligned} S_{\mathrm{hh}} &= 2R_{\perp}(0), \\ S_{\mathrm{vh}} &= -S_{\mathrm{hv}} = 0, \\ S_{\mathrm{vv}} &= 2R_{/\!/}(0), \end{aligned} \tag{55}$$

which confirms the results found in [*Franceschetti et al.*, 2002] [see (4.6a-4.6c)] apart for a sign change in S_{hh} and S_{hv}, due to the different conventions used for the evaluation of the scattering matrix [*Lee and Pottier*, 2009]. As expected from the KA-GO approximation, the cross-polarized backscattered coefficients are zero [*Franco et al.*, 2017].

6.2.2 KA-PO

Under the KA-PO approximation, the backscattering from wall is given either by (50) for $\theta_{\mathrm{n}}=\pi/2$, or by (43) for $\theta_{\mathrm{n}}=\pi/2$ upon substitution of (53). It then results

$$\begin{aligned} S_{\mathrm{hh}} &= U_0[R_{\perp}(\psi)\cos^2\theta_{\mathrm{i}}\cos^2(\phi_{\mathrm{i}}-\phi_{\mathrm{n}}) - R_{/\!/}(\psi)\sin^2(\phi_{\mathrm{i}}-\phi_{\mathrm{n}})], \\ S_{\mathrm{vh}} &= -\tilde{S}_{\mathrm{hv}} = U_0\sin(\phi_{\mathrm{i}}-\phi_{\mathrm{n}})[R_{\perp}(\psi)+R_{/\!/}(\psi)], \\ S_{\mathrm{vv}} &= U_0[R_{\perp}(\psi)\sin^2(\phi_{\mathrm{i}}-\phi_{\mathrm{n}}) - R_{/\!/}(\psi)\cos^2\theta_{\mathrm{i}}\cos^2(\phi_{\mathrm{i}}-\phi_{\mathrm{n}})], \end{aligned} \tag{56}$$

with $U_0 = 2\sin\theta_{\mathrm{i}}\cos(\phi_{\mathrm{i}}-\phi_{\mathrm{n}})/[1-\sin^2\theta_{\mathrm{i}}\cos^2(\phi_{\mathrm{i}}-\phi_{\mathrm{n}})]$. Equation (56) confirms the results found in [*Franceschetti et al.*, 2002] [see (4.2a)–(4.2.c)] according to the definitions in (52) and apart for the sign change in S_{hh} and S_{hv} (for the same motivations as above). As opposed to KA-GO, KA-PO does not generally lead to zero cross-polarized backscattered power, as recently shown in [*Franco et al.*, 2017].

With regard to the backscattering from ground, S_{pq} is given either by (50) for $\theta_{\mathrm{n}}=0$, or by (47) for $\theta_{\mathrm{n}}=0$ upon subsitution of (53). Thus, it is easily found that

$$\begin{aligned} S_{\mathrm{hh}} &= -2R_{\perp}(\pi-\theta_{\mathrm{i}})\cos\theta_{\mathrm{i}}, \\ S_{\mathrm{vh}} &= -S_{\mathrm{hv}} = 0, \\ S_{\mathrm{vv}} &= -2R_{/\!/}(\pi-\theta_{\mathrm{i}})\cos\theta_{\mathrm{i}}, \end{aligned} \tag{57}$$

which again confirms the results found in [*Franceschetti et al.*, 2002] [see (4.9a-4.9c)] according to the definitions in (52) and apart for the abovementioned sign change.

As a final comment, we note that the S^0_{pq} term appearing under the KA-PO approximation vanishes under the BS hypothesis.

7 Canonical Study Cases

In this Section, the developed theoretical framework for the evaluation of the scattering matrix under KA is exploited to clarify the benefits of the proposed formalism for the study of electromagnetic problems of practical interests. In particular, we show that the formulas provided in the previous sections can greatly simplify the theoretical derivation of the scattering matrix in scenarios with composite targets, where multiple-bounce contributions arise due to multiple reflections. Two canonical study cases are presented here: the backscattering from a smooth parallelepiped target lying on a rough surface (Subsection 7.1) and the backscattering from a rough square pyramid on a horizontal rough surface (Subsection 7.2).

7.1 Parallelepiped Target

Here we analyze the canonical problem depicted in Fig. 2, consisting of a smooth parallelepiped target lying on a rough surface. Such a study case has been analyzed in

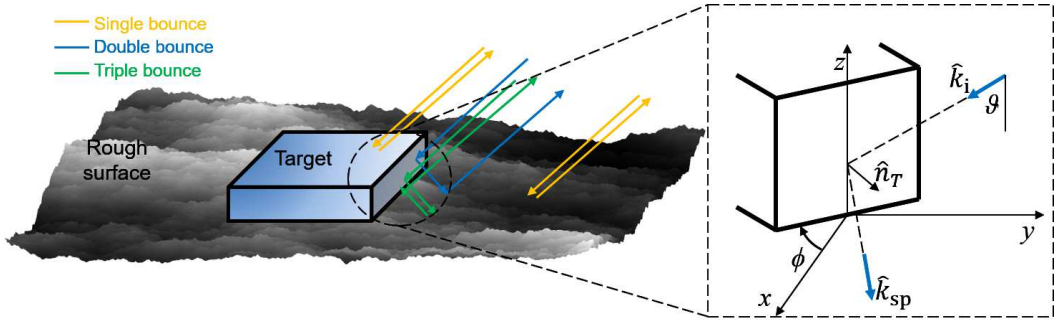

Figure 2. Canonical problem of a composite target consisting of a smooth parallelepiped lying on a rough surface. Single-bounce (yellow), double-bounce (blue), and triple-bounce (green) scattering contributions. The geometry of the double-bounce contribution is shown in the inset.

both urban and maritime environments to derive the analytical expression of the RCS of an isolated building and vessel in a backscattering configuration under KA-GO and KA-PO [*Franceschetti et al.*, 2002; *Iervolino et al.*, 2016]. For the theoretical evaluation of the electromagnetic field scattered from such a target, it is convenient to decompose the scattered field in the different contributions arising from multiple reflections between the target and the surface. Such terms can then be evaluated by means of KA-GO and KA-PO as demonstrated in [*Franceschetti et al.*, 2002]. In the considered problem, the following contributions are present (see Fig. 2):

- Single-bounce scattering from rough surface and target (yellow lines).
- Double-bounce scattering from target-surface and vice versa (blue lines).
- Triple-bounce scattering from target-surface-target (green lines).

Single-bounce contributions can be easily evaluated by means of well-known theory of scattering from rough surfaces [*Tsang and Kong*, 2001; *Barrick*, 1970; *Bass and Fuks*, 1979]. However, once the acquisition geometry is known, the single-bounce contributions can easily be evaluated through the application of *i)* (32)-(34) along with symmetries in (35), for KA, *ii)* (40) and (41) for KA-GO, and *iii)* (47) for KA-PO. Therefore, we here focus on the target-surface double-bounce contribution and illustrate the rationale to derive the analytical expression of the scattering matrix under KA-GO. A similar procedure can be applied to evaluate the scattering matrix of the surface-target and target-surface-target scattering terms under either KA-GO or KA-PO. Assuming the geometry shown in Fig. 2, the incident field $\underline{E}_i$ can be modeled as a plane wave with amplitude E_0, polarization $\hat{e}_i$ and propagating in the $\hat{k}_i$ direction [*Franceschetti et al.*, 2002]. It is here assumed that $\hat{k}_i$ lays in the yz plane, therefore:

$$\hat{k}_i = -\sin\theta\hat{y} - \cos\theta\hat{z}, \tag{58}$$

where θ is the radar look angle.

From (12), with the definitions in (5a) and (5b), it is evident that the scattering matrix is a function of the propagation and observation directions, and unit vector normal to the surface, i.e., $\underline{\underline{S}} = \underline{\underline{S}}(\hat{k}_i, \hat{k}_s, \hat{n})$. Under KA-GO, the electric field scattered from the target is still a plane wave propagating along the direction [*Franceschetti et al.*, 2002]

$$\hat{k}_{sp} = \sin\theta\sin 2\phi\hat{x} + \sin\theta\cos 2\phi\hat{y} - \cos\theta\hat{z} \tag{59}$$

Therefore, the scattering matrix associated to the first bounce is

$$\underline{\underline{S}}_{\mathrm{T}} = \underline{\underline{S}}(\hat{k}_{\mathrm{i}}, \hat{k}_{\mathrm{sp}}, \hat{n}_{\mathrm{T}}) \tag{60}$$

where $\hat{n}_{\mathrm{T}} = \sin\phi\hat{x} + \cos\phi\hat{y}$, and (37), (38) can be directly applied. In order to provide an analytical expression of the scattering matrix in terms of the incident and scattering angles, (39) provides the formal changes to be applied to (40) and (41):

$$\begin{aligned} \theta_{\mathrm{i}} &= \pi - \theta, \\ \phi_{\mathrm{i}} &= -\pi/2, \\ \theta_{\mathrm{s}} &= \pi - \theta, \\ \phi_{\mathrm{s}} &= \pi/2 - 2\phi. \end{aligned} \tag{61}$$

The scattering matrix for the bounce from the surface is:

$$\underline{\underline{S}}_{\mathrm{S}} = \underline{\underline{S}}(\hat{k}_{\mathrm{sp}}, \hat{k}_{\mathrm{s}}, \hat{n}_{\mathrm{S}}) \tag{62}$$

since the incident plane wave is now propagating along the $\hat{k}_{\mathrm{sp}}$ direction. The unit vector $\hat{n}_{\mathrm{S}}$ is determined by (14). Similarly, the analytical expression of $\underline{\underline{S}}_{\mathrm{S}}$ in terms of angles can be derived from the following formal changes:

$$\begin{aligned} \theta_{\mathrm{i}} &= \pi - \theta, \\ \phi_{\mathrm{i}} &= \pi/2 - 2\phi, \\ \theta_{\mathrm{s}} &= \theta_{\mathrm{s}}, \\ \phi_{\mathrm{s}} &= \phi_{\mathrm{s}}, \end{aligned} \tag{63}$$

Finally, the overall scattering matrix of the double-bounce target-surface contribution $\underline{\underline{S}}_{\mathrm{TS}}$ can be obtained as:

$$\underline{\underline{S}}_{\mathrm{TS}} = \underline{\underline{S}}_{\mathrm{S}} \underline{\underline{S}}_{\mathrm{T}}. \tag{64}$$

We note that (64) can suitably be generalized for N-th order multiple-bounce contributions: if $\underline{\underline{S}}_{\mathrm{U}}^{(i)}$ for $i = 1, 2, \ldots N$ is the single-bounce scattering matrix of the i-th bounce, the overall scattering matrix relevant to the N-th order contribution $\underline{\underline{S}}_{\mathrm{C}}$ is given by the non-commutative product:

$$\underline{\underline{S}}_{\mathrm{C}} = \prod_{i=1}^{N} \underline{\underline{S}}_{\mathrm{U}}^{(N+1-i)}. \tag{65}$$

Even more interestingly we note that the scattering matrix of a composite target inherits the duality and reciprocity symmetries of the single-bounce scattering matrix (see (35)), as rigorously shown in the Appendix.

With these considerations at hand, we show numerical results of the bistatic RCS of the double-bounce target-surface contribution arising in the canonical problem presented in Fig. 2. We note here that under KA-GO and KA-PO approximations, the scattered fields and in turn the RCS are given by (9). Therefore, once the scattering matrix of the composite target is calculated as shown in (65), only the surface integrals I_{S} have to be computed to obtain the bistatic RCS. While analytical expressions of I_{S} can be found under specific hypotheseis, their calculation is here performed through numerical techniques. The scattering integral I_S over the sea surface has been evaluated by means of a Monte Carlo simulation with 10^6 trials .

The simulated scenario is a maritime environment where a $100 \times 30 \times 10$ m^3 ship target lays on the sea surface described via a 2-D Gaussian stochastic process with standard

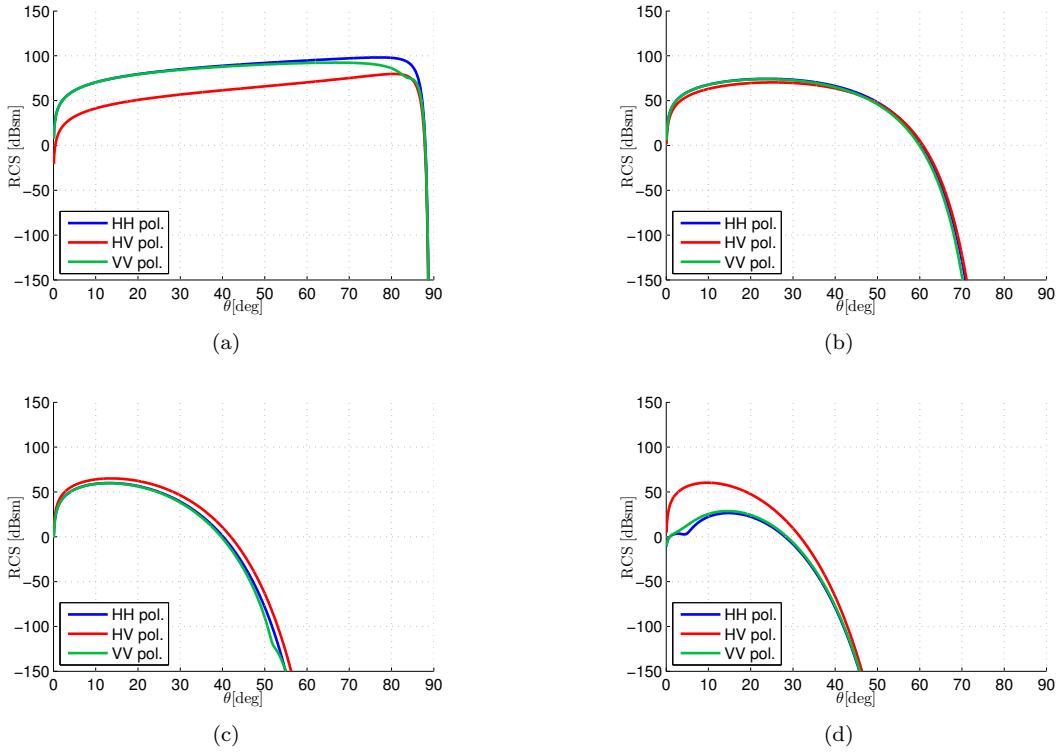

Figure 3. Backscattering RCS of the ship target at 3 GHz for (a) $\phi = 0°$, (b) $\phi = 15°$, (c) $\phi = 30°$, (d) $\phi = 45°$. Only the double-bounce ship-sea is modeled.

deviation 0.1 m. The Klein-Swift model in [*Klein and Swift*, 1977] is used to evaluate the sea dielectric constant. To this end, sea salinity and temperature are set to 35 ppm and 19°, respectively. The operating frequency is set to 3 GHz, and radar look angle to 30°, unless otherwise stated.

Figures 3(a)-(d) show the RCS in the backscattering configuration as a function of the radar look angle θ for linear co-pol HH, VV, and cross-pol HV polarizations and for $\phi = 0°$ (long side of ship facing the transmitter), $\phi = 15°$, $\phi = 30°$, and $\phi = 45°$. It is worth noting that similar results are expected with larger values of the aspect angle ϕ due to the symmetry of the target. For low aspect angles, the cross-pol channel exhibits the lowest RCS values, whereas the highest RCS values are achieved for large aspect angles. Co-pol channels give similar results in the considered scenario. Figures 4(a)-(d) show the bistatic RCS as a function of ϕ_s for $\phi = 0°$, $\phi = 15°$, $\phi = 30°$, and $\phi = 45°$. The double-bounce contributions from the different ship sides appear as local peaks of the RCS, with angular position dictated by the ship orientation. Finally, it is demonstrated that, for a large range of ship orientations, the backscattering acquisition geometry represents the most favorable configuration for ship detection applications in bistatic systems, such as GNSS-R.

7.2 Pyramidal Target

As a further canonical study case, we analyze the composite scenario depicted in Fig. 5(a). It consists of a square right pyramid with rough sides lying on a rough horizontal surface. Such a study case is not only important *per se*, but allows us for considering a more generic scenario with respect to the parallelepiped target considered in the previous section. Actually, in this case we consider tilted facets, thus paving the way for the electromagnetic

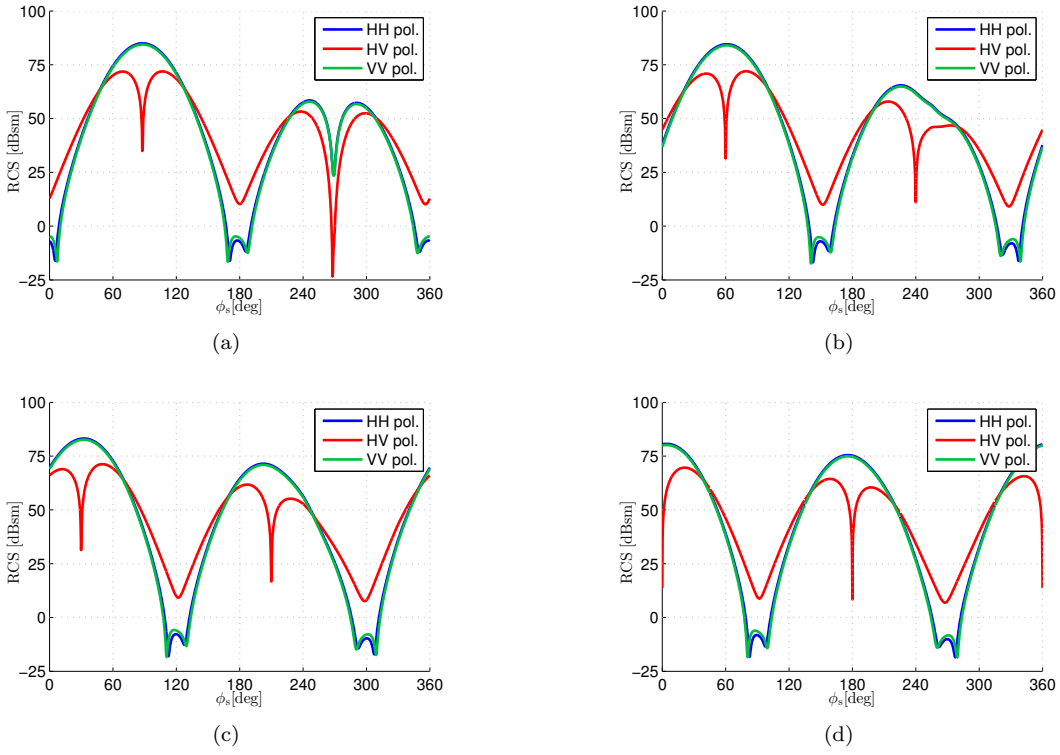

738 **Figure 4.** RCS of the ship target at 3 GHz and $\theta = 30°$ as a function of ϕ_s for (a) $\phi = 0°$, (b)
739 $\phi = 15°$, (c) $\phi = 30°$, (d) $\phi = 45°$. Only the double-bounce ship-sea is modeled.

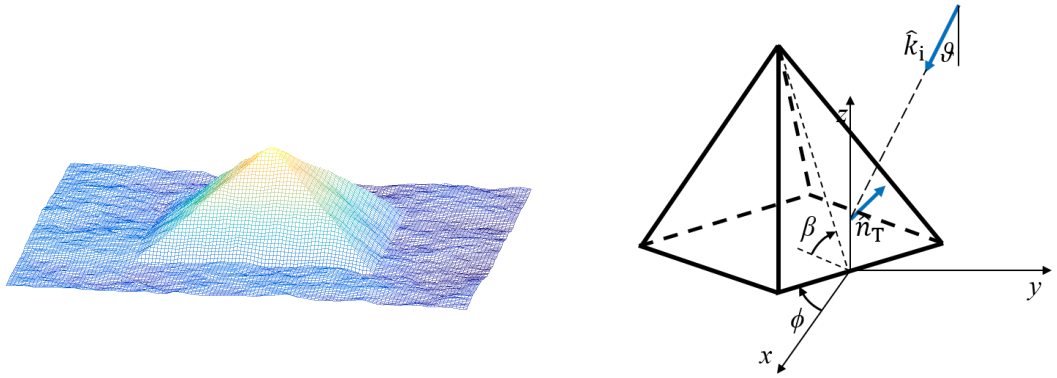

758 **Figure 5.** (a) Composite scenario consisting in a square right pyramid with rough sides lying
759 on a rough horizontal surface. (b) Geometry of the problem.

766 modeling of targets which significantly differ from parallelepiped, e.g., small ships, gable-
767 roofed buildings. Here we show how the scattering matrix relevant to the single-scattering
768 contribution from the slant face of the pyramid can be derived by using the proposed formu-
769 las. In particular, we consider a monostatic radar system illuminating the whole composite
770 surface and analyze the scattering problem in the framework of the KA-PO approach. The
771 unit vector normal to the slant face can then be expressed as:

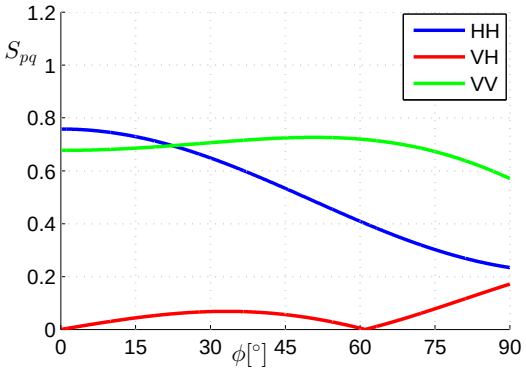

Figure 6. S_{pq} relevant to the single-scattering contribution from pyramid as a function of the pyramid aspect angle ϕ for HH (blue line), VV (green), and VH (red line). The pyramid slant angle and radar look angle are $\beta = 50°$ and $\theta = 30°$, respectively.

$$\hat{n}_{\mathrm{T}} = \sin\beta\sin\phi\hat{x} + \sin\beta\cos\phi\hat{y} + \cos\beta\hat{z} \tag{66}$$

where ϕ is the clockwise angle between the x-axis and pyramid line base and β is the slant angle, i.e., the angle between the slant face and the base, see Fig. 5(b). The scattering matrix relevant to the single-scattering contribution from the slant face can be derived by using (50) and (51) with the same substitutions and angle definitions in (52) and $\theta_{\mathrm{n}} = \beta$. It results that:

$$\begin{aligned}
S_{\mathrm{hh}} &= \frac{2\cos\psi}{\sin^2\psi}[+R_{\perp}(\psi)(\sin\theta\cos\beta - \cos\theta\sin\beta\cos\phi)^2 - R_{/\!/}(\psi)\sin^2\beta\sin^2\phi], \\
S_{\mathrm{vh}} &= -S_{\mathrm{hv}} = \frac{2\cos\psi}{\sin^2\psi}[R_{\perp}(\psi) + R_{/\!/}(\psi)]\sin\beta\sin\phi(\sin\theta\cos\beta - \cos\theta\sin\beta\cos\phi), \\
S_{\mathrm{vv}} &= \frac{2\cos\psi}{\sin^2\psi}[-R_{\perp}(\psi)\sin^2\beta\sin^2\phi + R_{/\!/}(\psi)(\sin\theta\cos\beta - \cos\theta\sin\beta\cos\phi)^2],
\end{aligned} \tag{67}$$

where ψ can be expressed as:

$$\psi = \arccos(\sin\theta\sin\beta\cos\phi + \cos\theta\cos\beta). \tag{68}$$

In the limiting case $\beta = \theta$ and $\phi = 0$, $\psi = 0$ and (67) can be rewritten as:

$$\begin{aligned}
S_{\mathrm{hh}} &= 2R_{\perp}, \\
S_{\mathrm{vh}} &= -S_{\mathrm{hv}} = 0, \\
S_{\mathrm{vv}} &= 2R_{/\!/}.
\end{aligned} \tag{69}$$

It is worth mentioning that such results generalize the scattering matrix reported in [[*Franceschetti et al.*, 2002], Table I] to tilted walls.

Numerical results showing the scattering matrix in (67) relevant to the single-scattering contribution from the pyramid target are here presented and discussed. The simulated target exhibits a dielectric constant equal to 5; the pyramid slant angle and the radar look angle are $\beta = 50°$ and $\theta = 30°$, respectively, unless otherwise stated.

Fig. 6 shows the scattering matrix elements as a function of the pyramid aspect angle ϕ for the different co-pol and cross-pol channels. Due to the symmetry of the target, only aspect angles in the range $0° < \phi < 90°$ have been considered. In this way, all the possible orientations are represented. At low aspect angles, S_{hh} exhibits the largest values,

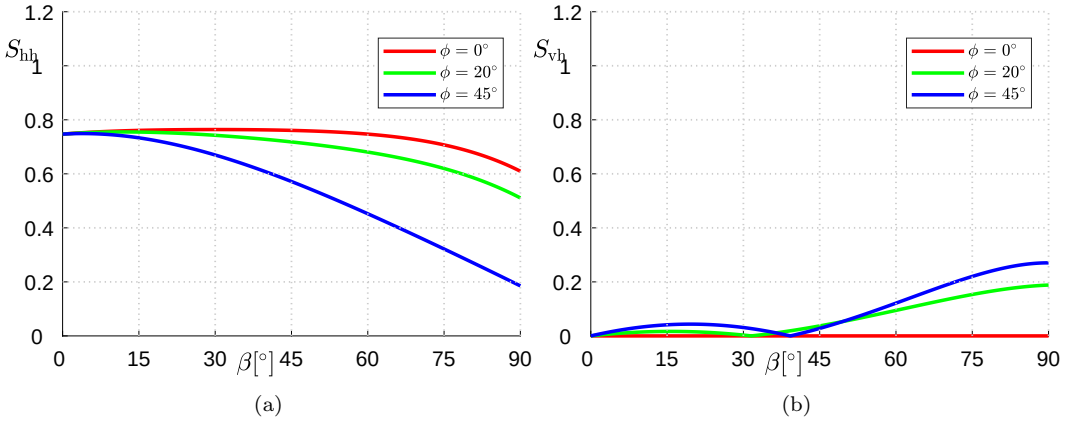

Figure 7. S_{pq} relevant to the single-scattering contribution from a pyramid as a function of the pyramid slant angle β for $\phi = 0°$ (red line), $\phi = 20°$ (green line), and $\phi = 45°$ (blue line). (a) $S_{\rm hh}$, (b) $S_{\rm vh}$. The radar look angle is $\theta = 30°$.

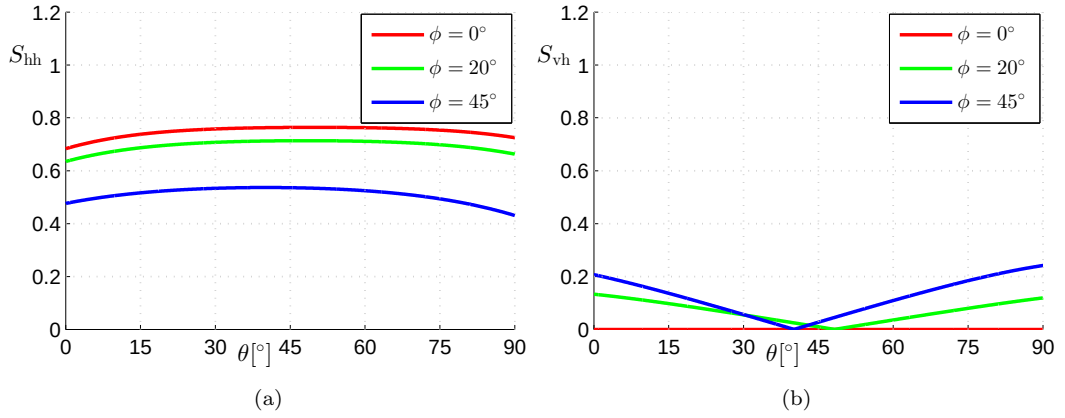

Figure 8. S_{pq} relevant to the single-scattering contribution from pyramid as a function of the radar look angle θ for $\phi = 0°$ (red line), $\phi = 20°$ (green line), and $\phi = 45°$ (blue line). (a) $S_{\rm hh}$, (b) $S_{\rm vh}$. Pyramid slant angle is $\beta = 50°$.

whereas at intermediate and large aspect angles $S_{\rm vv}$ dominates. The cross-pol channels give the lowest values, regardless of the target orientation, and present nulls for $\phi = 0°$ and $\phi = \arccos(\tan\theta\cot\beta)$, which corresponds to about 60° in the considered scenario. The role of the pyramid slant angle β is investigated in Fig. 7, which shows $S_{\rm hh}$ and $S_{\rm vh}$ as a function of β for different aspect angles. Results analogous to $S_{\rm hh}$ ($S_{\rm vh}$) have been obtained for $S_{\rm vv}$ ($S_{\rm hv}$) and, therefore, are omitted here. It is obvious that, for null slant angle, the scattering matrix no longer depends upon the pyramid aspect angle β, as is confirmed in Fig. 7. Indeed, $S_{\rm hh}$ is a decreasing function of β and its sensitivity to the slant angle β increases with increasing aspect angle ϕ. Regardless of the slant angle, the cross-pol channels are null for target in broadside configuration, i.e., $\phi = 0$, as mentioned before. Further nulls are for $\beta = 0°$ and $\beta = \arctan(\tan\theta/\cos\phi)$, corresponding to about 31° and 39° for $\phi = 20°$ and $\phi = 45°$, respectively. $S_{\rm hv}$ increases stepping away from such values, reaching largest values for large aspect angle ϕ.

Finally, we analyze the role of the radar look angle θ. Results are presented in Fig. 8, where $S_{\rm hh}$ and $S_{\rm vh}$ are shown as a function of θ for different aspect angles ϕ. It is demon-

strated that $S_{\rm hh}$ is weakly influenced by the radar look angle θ at any target orientation, and largest values are achieved with broadside targets. Similar comments to Fig. 7(b) can be applied to Fig. 8(b) concerning $S_{\rm vh}$. However, a unique null in $\theta = \arctan(\tan\beta\cos\phi)$ is found in terms of θ.

As a last remark, it is worth commenting here that the presence of nulls in the cross-pol channels can easily be predicted from (67). This aspect further corroborates the advantages in having analytic closed-form expressions for the scattering matrix coefficients in terms of angles.

8 Comparison with Results from the Literature

In this Section, the proposed framework is validated against literature results. First, we compare the proposed method with the one presented in [*Arnold-Bos et al.*, 2007a] in order to assess the consistency of our analytical derivation. Second, we compare our analytical results with those obtained with the facet-based approach (FBA) presented in [*Chen et al.*, 2012].

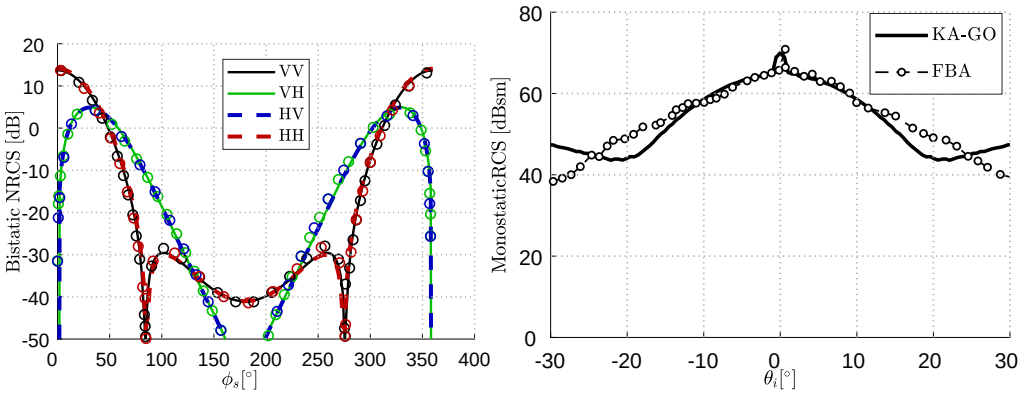

(a) (b)

Figure 9. (a) Normalized RCS vs. ϕ_s, of a rough sea surface for $f_0 = 10$ GHz, wind speed equal to 4.53 m/s, $\theta = 20°$, $\theta_{\rm s} = 30°$, $\phi_{\rm i} = 0°$. Our results are in solid and dashed lines, while results taken from [*Arnold-Bos et al.*, 2007a] are in circles. (b) Monostatic RCS vs. $\theta_{\rm i}$ for the composite scattering of a ship (see [*Chen et al.*, 2012] for the ship model) lying on a rough sea surface at $f = 8$ GHz and HH polarization. The sea surface is characterized by a JONSWAP spectrum [*Hasselmann et al.*, 1980] assuming a wind speed of 4 m/s. Our results are in black solid line, while the FBA results taken from [*Chen et al.*, 2012] are in black circles. Note that we modeled the ship as an equivalent parallelepiped of dimensions $120 \times 20 \times 25$ m^3.

8.1 Validation of the Analytical Derivation

In order to prove the consistency of the proposed analytical derivation, it is important to compare our results with those obtained by means of different methods but still under the same approximation. In this regard, the numerical results obtained in [*Arnold-Bos et al.*, 2007a] for the normalized radar cross section (NRCS) of a rough sea surface are reported in Fig. 9(a) where those results are compared with ours under the same approximation (i.e., KA-GO) and operating conditions (parameters in the caption of Fig. 9(a)). As expected, our KA-GO formulation leads to the same results of [*Arnold-Bos et al.*, 2007a] (the negligible differences between the two figures are due to slightly different statistical characterization

of the sea surface roughness), but with the difference that our results are obtained by means of fully analytical explicit expressions (see (40)). As extensively discussed in [*Arnold-Bos et al.*, 2007a], we should mention that the KA-GO approximation provides accurate results in the specular region (i.e., $\phi_s \in [0°, 20°] \cup [340°, 360°]$), while it generally underrates diffuse scattering (i.e., $\phi_s > 20°$).

8.2 Validation with Numerical Models

At this stage, it is important to compare the accuracy of our results with other numerical techniques. In this regard, the KA-GO framework proposed here for the evaluation of the RCS is compared with the FBA method presented in [*Chen et al.*, 2012]. The FBA is a reliable method in the family of facet-based algorithms (see, e.g., [*Chen et al.*, 2009, 2012; *Zhang et al.*, 2017, 2011]), the latter being semi-analytical hybrid schemes recently introduced to improve the efficiency of computationally expensive full-wave techniques, such as the multilevel fast multipole method (MLFMM) (see e.g., [*Sertel and Volakis*, 2004]). In particular, in [*Chen et al.*, 2012] a hybrid method which combines the GO-PO solution with the method of equivalent currents (MEC), is proposed as a convenient numerical tool for evaluating the RCS of an isolated target lying over a rough surface.

Here, we compare our results with those obtained in [*Chen et al.*, 2012] for evaluating the monostatic RCS (i.e., backscattering configuration) of a ship lying over a moderately rough sea (parameters in the caption of Fig. 9(b)). As shown in Fig. 9(b), our KA-GO solution (black solid line) exhibits a good agreement with the numerical results (black circles) reported in [*Chen et al.*, 2012]. We limited our analysis to $0° < \theta_i < 30°$, as the KA-GO approximation is not expected to give accurate results for larger incidence angles. Incidentally, we stress here that this variability range is in accordance with typical viewing angles adopted in remote sensing technologies, such as SAR, scatterometers, and GNSS-R, which typically exhibit a viewing angle up to few tens of degrees. As a final remark, we should emphasize that our analytical KA-GO framework, although modeling the ship as a simple parallelepiped, is still able of providing a good estimate of the main scattering mechanisms at very low computational cost compared with numerical techniques. Indeed, FBA methods always require the discretization of the entire scenario (i.e., the rough sea surface as well as the ship) in a multitude of facets, thus demanding high memory and time resources when dealing with surfaces much larger than facets, as those reported here.

9 Conclusion

In this work we have presented an alternative theoretical derivation of the scattering matrix under the Kirchhoff approximation (KA), where no simplifying assumptions have been made about the scattering geometry. Special emphasis is devoted to the backscattering case because of its relevance to remote sensing. The proposed formalism highlights interesting symmetries of the scattering matrix under KA, and enables a straightforward derivation of analytical expressions under the geometrical optics (KA-GO) and the physical optics (KA-PO) approximations. In addition, these formulas are explicitly expressed in terms of either the unit wavevectors and surface orientation, or the relative positions between the transmitter, the scatterer, and the receiver. The proposed theoretical framework paves the way for a direct evaluation of the electromagnetic field scattered from composite targets, simplifying the theoretical derivation of the scattering matrix. This has been demonstrated in two canonical examples of practical interest, where the problem of the EM scattering from composite targets has been analyzed. In the first canonical study case, consisting of a parallelepiped target lying over a rough surface, the rationale for evaluating the overall bistatic scattering matrix associated to a double-bounce term has been formulated under KA-GO. In the second application example, the monostatic scattering matrix associated to a single-bounce from tilted facets has been derived under KA-PO. The presented formulas allow us to evaluate the role of the target geometry on the scattering matrix. By accounting for

such scattering contributions, numerical results have been presented and discussed. Finally, the proposed analytical framework has been validated against both analytical models and simulation tools available in the literature in order to validate the whole analytical derivation, and to test its accuracy and validity limits as opposed to numerical techniques. The comparisons have highlighted both the consistency of the proposed analytical framework and its accuracy in realistic scenarios for low to intermediate viewing angles.

A: Duality and Symmetry Properties of the Scattering Matrix from Multiple Bounces

We want to prove that (35) holds also for the scattering matrix of the N-th order multiple-bounce contributions, i.e.,

$$\begin{aligned} S_{\mathrm{C,vv}}(\underline{R}_{\perp},\underline{R}_{/\!/}) &= S_{\mathrm{C,hh}}(\underline{R}_{/\!/},\underline{R}_{\perp}),\\ S_{\mathrm{C,hv}}(\underline{R}_{\perp},\underline{R}_{/\!/}) &= -S_{\mathrm{C,vh}}(\underline{R}_{/\!/},\underline{R}_{\perp}), \end{aligned} \tag{A.1}$$

where $S_{\mathrm{C,pq}}$, for $p,q\in\{\mathrm{h},\mathrm{v}\}$ is the pq-component of $\underline{\underline{S}}_{\mathrm{C}}$ in (65) for N bounces, whereas $\underline{R}_{/\!/}=[R_{/\!/,1},R_{/\!/,2},\ldots,R_{/\!/,N}]$, $\underline{R}_{\perp}=[R_{\perp,1},R_{\perp,2},\ldots,R_{\perp,N}]$, represent the N-tuples of Fresnel coefficients, with $R_{/\!/,i}$ and $R_{\perp,i}$ for $i=1,2,\ldots,N$ their Fresnel coefficients of the i-th bounce, for locally parallel and perpendicular polarizations, respectively.

Mathematical induction can profitably be used to prove (A.1). Indeed, the basis of induction is already proven, as we know that equation (35) holds for the single-scattering event (i.e., for $N=1$). Hence, only the inductive step remains to prove. First, we define $\underline{\underline{S}}_{\mathrm{C}}^{(n)}$, and $\underline{R}_{/\!/}^{(n)}$, and $\underline{R}_{\perp}^{(n)}$, the composite scattering matrix and the tuples of parallel and perpendicular Fresnel coefficients, respectively, for $n\in\mathbb{N}^*$ bounces. By induction hypothesis, we then assume that (A.1) holds for $\underline{\underline{S}}_{\mathrm{C}}^{(n)}$. From (65) we have that $\underline{\underline{S}}_{\mathrm{C}}^{(n+1)}=\underline{\underline{S}}_{\mathrm{U}}^{(n+1)}\underline{\underline{S}}_{C}^{(n)}$, with $\underline{\underline{S}}_{\mathrm{U}}^{(n+1)}$ the single-bounce scattering matrix of the $n+1$-th bounce. Therefore,

$$\begin{aligned} S_{\mathrm{C,hh}}^{(n+1)} &= S_{\mathrm{U,hh}}^{(n+1)}S_{\mathrm{C,hh}}^{(n)}+S_{\mathrm{U,vh}}^{(n+1)}S_{\mathrm{C,hv}}^{(n)},\\ S_{\mathrm{C,vh}}^{(n+1)} &= S_{\mathrm{U,hh}}^{(n+1)}S_{\mathrm{C,vh}}^{(n)}+S_{\mathrm{U,vh}}^{(n+1)}S_{\mathrm{C,vv}}^{(n)},\\ S_{\mathrm{C,hv}}^{(n+1)} &= S_{\mathrm{U,hv}}^{(n+1)}S_{\mathrm{C,hh}}^{(n)}+S_{\mathrm{U,vv}}^{(n+1)}S_{\mathrm{C,hv}}^{(n)},\\ S_{\mathrm{C,vv}}^{(n+1)} &= S_{\mathrm{U,hv}}^{(n+1)}S_{\mathrm{C,vh}}^{(n)}+S_{\mathrm{U,vv}}^{(n+1)}S_{\mathrm{C,vv}}^{(n)}, \end{aligned} \tag{A.2}$$

where the dependence of $\underline{\underline{S}}_{\mathrm{U}}^{(n+1)}$ from $R_{/\!/,n+1}$ and $R_{\perp,n+1}$, and that of $\underline{\underline{S}}_{\mathrm{C}}^{(n)}$ from $\underline{R}_{/\!/}^{(n)}$ and $\underline{R}_{\perp}^{(n)}$, have been tacitly suppressed for clarity purposes. Since $\underline{\underline{S}}_{\mathrm{C}}^{(n+1)}$ depends on both $\underline{R}_{/\!/}^{(n)}$, $\underline{R}_{\perp}^{(n)}$, and $R_{/\!/,n+1}$, $R_{\perp,n+1}$, it is convenient to define the $n+1$-tuples of Fresnel coefficients as $\underline{R}_{/\!/(\perp)}^{(n+1)}=[\underline{R}_{/\!/(\perp)}^{(n)},R_{/\!/(\perp),n+1}]$. With this definition at hand, and by exploiting the induction hypothesis on $\underline{\underline{S}}_{\mathrm{C}}^{(n)}$ and (A.1) on $\underline{\underline{S}}_{\mathrm{U}}^{(n+1)}$, it is straightforward to show that:

$$\begin{aligned} &S_{\mathrm{U,hh}}^{(n+1)}(R_{/\!/,n+1},R_{\perp,n+1})S_{\mathrm{C,hh}}^{(n)}(\underline{R}_{/\!/}^{(n)},\underline{R}_{\perp}^{(n)})+S_{\mathrm{U,vh}}^{(n+1)}(R_{/\!/,n+1},R_{\perp,n+1})S_{\mathrm{C,hv}}^{(n)}(\underline{R}_{/\!/}^{(n)},\underline{R}_{\perp}^{(n)})=\\ &S_{\mathrm{U,vv}}^{(n+1)}(R_{\perp,n+1},R_{/\!/,n+1})S_{\mathrm{C,vv}}^{(n)}(\underline{R}_{\perp}^{(n)},\underline{R}_{/\!/}^{(n)})S_{\mathrm{U,hv}}^{(n+1)}(R_{\perp,n+1},R_{/\!/,n+1})S_{\mathrm{C,vh}}^{(n)}(\underline{R}_{\perp}^{(n)},\underline{R}_{/\!/}^{(n)}), \end{aligned} \tag{A.3}$$

and

$$\begin{aligned} &S_{\mathrm{U,hh}}^{(n+1)}(R_{/\!/,n+1},R_{\perp,n+1})S_{\mathrm{C,vh}}^{(n)}(\underline{R}_{/\!/}^{(n)},\underline{R}_{\perp}^{(n)})+S_{\mathrm{U,vh}}^{(n+1)}(R_{/\!/,n+1},R_{\perp,n+1})S_{\mathrm{C,vv}}^{(n)}(\underline{R}_{/\!/}^{(n)},\underline{R}_{\perp}^{(n)})=\\ &-S_{\mathrm{U,vv}}^{(n+1)}(R_{\perp,n+1},R_{/\!/,n+1})S_{\mathrm{C,hv}}^{(n)}(\underline{R}_{\perp}^{(n)},\underline{R}_{/\!/}^{(n)})-S_{\mathrm{U,hv}}^{(n+1)}(R_{\perp,n+1},R_{/\!/,n+1})S_{\mathrm{C,hh}}^{(n)}(\underline{R}_{\perp}^{(n)},\underline{R}_{/\!/}^{(n)}), \end{aligned} \tag{A.4}$$

so that:

$$\begin{aligned} S_{\mathrm{C,vv}}^{(n+1)}\left(\underline{R}_{\perp}^{(n+1)},\underline{R}_{/\!/}^{(n+1)}\right) &= S_{\mathrm{C,hh}}^{(n+1)}\left(\underline{R}_{/\!/}^{(n+1)},\underline{R}_{\perp}^{(n+1)}\right),\\ S_{\mathrm{C,hv}}^{(n+1)}\left(\underline{R}_{\perp}^{(n+1)},\underline{R}_{/\!/}^{(n+1)}\right) &= -S_{\mathrm{C,vh}}^{(n+1)}\left(\underline{R}_{/\!/}^{(n+1)},\underline{R}_{\perp}^{(n+1)}\right). \end{aligned} \tag{A.5}$$

By mathematical induction (A.5) holds for any finite $n \in \mathbb{N}^*$, and this concludes the proof. Hence, the symmetry properties of the scattering matrix for a single-bounce contribution can be straightforwardly extended to a composite target through (A.1).

Acknowledgments

This research has been founded by the Office of Naval Research under contract N00014-16-13157, and this support is acknowledged with thanks to John Tague and Michael Vaccaro. There is parallel support to ONR-Global. Numerical data were obtained through the methods explained in the text. Literature data were properly referenced, when used for comparison purposes. No other data were used in this paper.

References

Arnold-Bos, A., A. Khenchaf, and A. Martin (2007a), Bistatic radar imaging of the marine environment–Part I: Theoretical background, *IEEE Transactions on Geoscience and Remote Sensing*, *45*(11), 3372–3383.

Arnold-Bos, A., A. Khenchaf, and A. Martin (2007b), Bistatic radar imaging of the marine environment–Part II: Simulation and results analysis, *IEEE Transactions on Geoscience and Remote Sensing*, *45*(11), 3384–3396.

Barrick, D. E. (1968), Relationship between slope probability density function and the physical optics integral in rough surface scattering, *Proceedings of the IEEE*, *56*(10), 1728–1729.

Barrick, D. E. (1970), *Radar Cross Section Handbook*, vol. II, Plenumpress, New York, NY, USA.

Bass, F. G., and I. M. Fuks (1979), *Wave Scattering from Statistically Rough Surfaces*, Pergamon, New York, NY, USA.

Chen, H., M. Zhang, D. Nie, and H.-C. Yin (2009), Robust semi-deterministic facet model for fast estimation on em scattering from ocean-like surface, *Progress In Electromagnetics Research*, *18*, 347–363.

Chen, H., M. Zhang, and H.-C. Yin (2012), Facet-based treatment on microwave bistatic scattering of three-dimensional sea surface with electrically large ship, *Progress In Electromagnetics Research*, *123*, 385–405.

Cherniakov, M. (2008), *Bistatic Radars: Emerging Technology*, John Wiley & Sons, Hoboken, NJ, USA.

Clarizia, M. P., P. Braca, C. S. Ruf, and P. Willett (2015), Target detection using GPS signals of opportunity, in *2015 18th International Conference on Information Fusion (FUSION)*, pp. 1429–1436, Washington, DC, USA.

Colone, F., D. O'Hagan, P. Lombardo, and C. Baker (2009), A multistage processing algorithm for disturbance removal and target detection in passive bistatic radar, *IEEE Transactions on Aerospace and Electronic Systems*, *45*(2).

Di Martino, G., A. Di Simone, and D. Riccio (2018), Fractal-based local range slope estimation from single sar image with applications to sar despeckling and topographic mapping, *Remote Sensing*, *10*(8), 1294.

Di Simone, A., H. Park, D. Riccio, and A. Camps (2017), Sea target detection using spaceborne GNSS-R delay-doppler maps: Theory and experimental proof of concept using TDS-1 data, *IEEE Journal of Selected Topics in Applied Earth Observations and Remote Sensing*, *10*(9), 4237–4255, doi:10.1109/JSTARS.2017.2705350.

El-Ocla, H., and M. Tateiba (2008), Verification of shadow region effect on radar cross section of targets using physical optics method, *Progress In Electromagnetics Research*, *5*, 81–89.

Elfouhaily, T. M., C.-A. Guérin, et al. (2004), A critical survey of approximate scattering wave theories from random rough surfaces, *Waves in Random Media*, *14*(4), R1–R40.

Franceschetti, G. (2013), *Electromagnetics: Theory, Techniques, and Engineering Paradigms*, Springer Science & Business Media, New York, NY, USA.

Franceschetti, G., and R. Lanari (2018), *Synthetic Aperture Radar Processing*, CRC press, Boca Raton, FL, USA.

Franceschetti, G., and D. Riccio (2007), *Scattering, Natural Surfaces, and Fractals*, Academic Press, New York, NY, USA.

Franceschetti, G., A. Iodice, and D. Riccio (2002), A canonical problem in electromagnetic backscattering from buildings, *IEEE Transactions on Geoscience and Remote Sensing*, *40*(8), 1787–1801.

Franco, M., M. Barber, M. Maas, O. Bruno, F. Grings, and E. Calzetta (2017), Validity of the Kirchhoff approximation for the scattering of electromagnetic waves from dielectric, doubly periodic surfaces, *J. Opt. Soc. Am. A*, *34*(12), 2266–2277.

Garrison, J. L. (2016), A statistical model and simulator for ocean-reflected GNSS signals, *IEEE Transactions on Geoscience and Remote Sensing*, *54*(10), 6007–6019.

Giangregorio, G., M. di Bisceglie, P. Addabbo, T. Beltramonte, S. D'Addio, and C. Galdi (2016), Stochastic modeling and simulation of delay–doppler maps in GNSS-R over the ocean, *IEEE Transactions on Geoscience and Remote Sensing*, *54*(4), 2056–2069.

Griffiths, H. (2014), Passive bistatic radar, in *Academic Press Library in Signal Processing*, vol. 2, pp. 813–855, Elsevier, Waltham, MA, USA.

Harrington, R. F. (1961), *Time-Harmonic Electromagnetic Fields*, Mcgraw-Hill, New York, NY, USA.

Harrington, R. F. (1993), Field computation by moment methods, *Wiley-IEEE Press*.

Hasselmann, D., M. Dunckel, and J. Ewing (1980), Directional wave spectra observed during jonswap 1973, *Journal of Physical Oceanography*, *10*(8), 1264–1280.

Hentschel, K., and N. Y. Zhu (2016), *Gustav Robert Kirchhoff's Treatise On the Theory of light Rays(1882) English Translation, Analysis and Commentary*, World Scientific.

Iervolino, P., R. Guida, and P. Whittaker (2016), A model for the backscattering from a canonical ship in SAR imagery, *IEEE Journal of Selected Topics in Applied Earth Observations and Remote Sensing*, *9*(3), 1163–1175.

Jin, S., and A. Komjathy (2010), GNSS reflectometry and remote sensing: New objectives and results, *Advances in Space Research*, *46*(2), 111–117.

Jin, S., G. Feng, and S. Gleason (2011), Remote sensing using GNSS signals: Current status and future directions, *Advances in Space Research*, *47*(10), 1645–1653.

Jin, Y.-Q., and M. Lax (1990), Backscattering enhancement from a randomly rough surface, *Phys. Rev. B*, *42*(16), 9819.

Klein, L., and C. Swift (1977), An improved model for the dielectric constant of sea water at microwave frequencies, *IEEE Journal of Oceanic Engineering*, *2*(1), 104–111.

Lee, J.-S., and E. Pottier (2009), *Polarimetric Radar Imaging: From Basics To Applications*, CRC press, Boca Raton, FL, USA.

Park, H., A. Camps, D. Pascual, Y. Kang, R. Onrubia, J. Querol, and A. Alonso-Arroyo (2017), A generic level 1 simulator for spaceborne GNSS-R missions and application to GEROS-ISS ocean reflectometry, *IEEE Journal of Selected Topics in Applied Earth Observations and Remote Sensing*, *10*(10), 4645–4659.

Pierdicca, N., L. Guerriero, R. Giusto, M. Brogioni, and A. Egido (2014), SAVERS: A simulator of GNSS reflections from bare and vegetated soils, *IEEE Transactions on Geoscience and Remote Sensing*, *52*(10), 6542–6554.

Sertel, K., and J. L. Volakis (2004), Multilevel fast multipole method solution of volume integral equations using parametric geometry modeling, *IEEE Transactions on Antennas and Propagation*, *52*(7), 1686–1692.

Stogryn, A. (1967), Electromagnetic scattering from rough, finitely conducting surfaces, *Radio Science*, *2*(4), 415–428.

Tateiba, M., Z. Q. Meng, and H. El-Ocla (2004), Scattering by conducting bodies in random media, *IEEJ Transactions on Fundamentals and Materials*, *124*(12), 1094–1100.

Tsang, L., and J. A. Kong (2001), *Scattering of Electromagnetic Waves: Advanced Topics*, John Wiley and Sons, New York, NY, USA.

Tsang, L., J. A. Kong, and R. T. Shin (1985), *Theory of Microwave Remote Sensing*, Wiley, New York, NY, USA.

Ulaby, F. T., R. K. Moore, and A. K. Fung (1982), *Microwave Remote Sensing*, vol. II, Artech House, Reading, MA, USA.

Zavorotny, V. U., and A. G. Voronovich (2000), Scattering of GPS signals from the ocean with wind remote sensing application, *IEEE Transactions on Geoscience and Remote Sensing*, *38*(2), 951–964.

Zavorotny, V. U., S. Gleason, E. Cardellach, and A. Camps (2014), Tutorial on remote sensing using GNSS bistatic radar of opportunity, *IEEE Geoscience and Remote Sensing Magazine*, *2*(4), 8–45.

Zhang, M., H. Chen, and H.-C. Yin (2011), Facet-based investigation on EM scattering from electrically large sea surface with two-scale profiles: Theoretical model, *IEEE Transactions on Geoscience and Remote Sensing*, *49*(6), 1967–1975.

Zhang, M., Y. Zhao, J.-X. Li, and P.-B. Wei (2017), Reliable approach for composite scattering calculation from ship over a sea surface based on FBAM and GO-PO models, *IEEE Transactions on Antennas and Propagation*, *65*(2), 775–784.

Zuffada, C., Z. Li, S. V. Nghiem, S. Lowe, R. Shah, M. P. Clarizia, and E. Cardellach (2015), The rise of GNSS reflectometry for earth remote sensing, in *2015 IEEE International Geoscience and Remote Sensing Symposium (IGARSS)*, pp. 5111–5114, Milan, Italy.